

Color Superconductivity at Moderate Baryon Density

Mei Huang ^{*}

1. *Institute for Theoretical Physics, J.W.Goethe University, Frankfurt am Main, Germany*
 2. *Physics Department, Tsinghua University, Beijing, China*

Abstract

This article focuses on the two-flavor color superconducting phase at moderate baryon density. In order to simultaneously investigate the chiral phase transition and the color superconducting phase transition, the Nambu-Gorkov formalism is extended to treat the quark-antiquark and diquark condensates on an equal footing. The competition between the chiral condensate and the diquark condensate is analyzed. The cold dense charge neutral two-flavor quark system is investigated in detail. Under the local charge neutrality condition, the ground state of two-flavor quark matter is sensitive to the coupling strength in the diquark channel. When the diquark coupling strength is around the value obtained from the Fierz transformation or from fitting the vacuum bayron mass, the ground state of charge neutral two-flavor quark matter is in a thermal stable gapless 2SC (g2SC) phase. The unusual properties at zero as well as nonzero temperatures and the chromomagnetic properties of the g2SC phase are reviewed. Under the global charge neutrality condition, assuming the surface tension is negligible, the mixed phase composed of the regular 2SC phase and normal quark matter is more favorable than the g2SC phase. A hybrid nonstrange neutron star is constructed.

Typeset using REVTEX

^{*}E-mail: huang@th.physik.uni-frankfurt.de

Contents

I	Introduction	2
A	QCD phase structure	2
B	Color superconducting phases	3
II	Competition between the chiral and diquark condensates	8
A	The extended NJL model	9
B	Nambu-Gorkov propagator with chiral and diquark condensates	12
C	Gap equations	14
D	Derivation of the thermodynamic potential	16
E	Competition between the chiral and diquark condensates	18
III	The gapless 2SC phase	25
A	Thermodynamic potential of the neutral two-flavor quark system	26
B	Gap equations and number densities	30
C	The charge neutral ground state and the g2SC phase	32
D	The g2SC phase at nonzero temperatures	36
E	Chromomagnetic instability in the g2SC phase	41
IV	The mixed phase and nonstrange hybrid star	43
A	The mixed phase	43
B	Nonstrange hybrid star	46
V	Conclusion and outlook	50
VI	Acknowledgements	51
APPENDIXES		52
A	Fierz transformation	52
1	Fierz transformation in the quark-antiquark sector	53
2	Fierz transformation in the diquark sector	53
B	Charge conjugation	54

I. INTRODUCTION

A. QCD phase structure

Quantum Chromodynamics (QCD) is regarded as the fundamental theory of quarks and gluons. Its ultimate goal is to explain all strong interaction experiments at all energies, high and low. QCD is an asymptotically free theory [1]. At very high energies, interaction forces become weak, thus perturbation calculations can be used. The perturbative QCD predictions have been extensively confirmed by experiments, while QCD in the non-perturbative regime is still a challenge to theorists. The fundamental quarks and gluons of QCD have not been seen as free particles, but are always confined within hadrons. It is still difficult to construct the hadrons in terms of nearly massless quarks and gluons. The observed baryon spectrum indicates that the (approximate) chiral symmetry is spontaneously broken in the vacuum. As a result, the eight pseudoscalar mesons π , K and η are light pseudo-Nambu-Goldstone bosons, and the constituent quark obtains dynamical mass, which contributes to the baryon mass. Besides conventional mesons and baryons, QCD itself does not exclude the existence of the non-conventional states such as glueballs, hybrid mesons and multi-quark states [2]. Last year, pentaquarks, e.g., $\Theta^+(u^2 d^2 \bar{s})$ [3] with the mass $M = 1540 \pm 10$ MeV and $\Xi^{--}(s^2 d^2 \bar{u})$ [4] with $M = 1862 \pm 18$ MeV, were discovered in experiments. This has stirred a great interest of theorists to understand the structure of the pentaquarks [5–8] as well as other fundamental problems of QCD in the non-perturbative regime.

Since 1970s, people have been interested in QCD at extreme conditions. It is expected that the chiral symmetry can be restored, and quarks and gluons will become deconfined at high temperatures and/or densities [9–12]. Results from lattice show that the quark-gluon plasma (QGP) does exist. For the system with zero net baryon density, the deconfinement and chiral symmetry restoration phase transitions happen at the same critical temperature [13]. At asymptotically high temperatures, e.g., during the first microseconds of the “Big Bang”, the many-body system composed of quarks and gluons can be regarded as an ideal Fermi and Boson gas. It is believed that the “little Bang” can be produced in RHIC and LHC. Recently, it was shown that the new state of matter produced in RHIC is far away from the asymptotically hot QGP, but in a strongly coupled regime. This state is called strongly coupled quark-gluon plasma (sQGP). In this strong coupling system, the meson bound states still play an important role [14,15]. For most recent reviews about QGP, e.g., see Ref. [16–19].

Studying QCD at finite baryon density is the traditional subject of nuclear physics. The behaviour of QCD at finite baryon density and low temperature is central for astrophysics to understand the structure of compact stars, and conditions near the core of collapsing stars (supernovae, hypernovae). Cold nuclear matter, such as in the interior of a Pb nucleus, is at $T = 0$ and $\mu_B \simeq m_N = 940$ MeV. Emerging from this point, there is a first-order nuclear liquid-gas phase transition, which terminates in a critical endpoint at a temperature ~ 10 MeV [20]. If one squeezes matter further and further, nucleons will overlap. Quarks and gluons in one nucleon can feel quarks and gluons in other nucleons. Eventually, deconfinement phase transition will happen. Unfortunately, at the moment, lattice QCD is facing the “sign problem” at nonzero net baryon densities. Our understanding at finite baryon densities has to rely on effective QCD models. Phenomenological models indicated that, at

nonzero baryon density, the QGP phase and the hadron gas are separated by a critical line of roughly a constant energy density $\epsilon_{cr} \simeq 1 \text{ GeV/fm}^3$ [21].

In the case of asymptotically high baryon density, the system is a color superconductor. This was proposed 25 years ago by Frautschi [22] and Barrois [23]. Reaching this conclusion does not need any other knowledge, if one knows that one-gluon exchange between two quarks is attractive in the color antitriplet channel, and if one is also familiar with the theory of superconductivity, i.e., the Bardeen, Cooper, and Schrieffer (BCS) theory [24]. Based on the BCS scenario, if there is a weak attractive interaction in a cold Fermi sea, the system is unstable with respect to the formation of particle-particle Cooper-pair condensate in the momentum space. Detailed numerical calculations of color superconducting gaps were firstly carried out by Bailin and Love [25]. They concluded that the one-gluon exchange induces gaps on the order of 1 MeV at several times of nuclear matter density. This small gap has little effect on cold dense quark matter, thus the investigation of cold quark matter lay dormant for several decades. It was only revived recently when it was found that the color superconducting gap can be of the order of 100 MeV [26], which is two orders larger than early perturbative estimates in Ref. [25]. For this reason, the topic of color superconductivity stirred a lot of interest in recent years. For review articles on the color superconductivity, see for example, Refs. [16,27–33].

In this paper, I will focus on the color superconducting phase structure at intermediate baryon density regime based on my own experience. It is worth to mention that there is another good review article Ref. [32] in this regime from another point of view. The outline of this article is as follows: A brief overview of color superconducting phases is given in Sec. I B. In Sec. II, the generalized Nambu-Gorkov formalism is introduced to treat the chiral and diquark condensates on an equal footing, and the competition between the chiral and color superconducting phase transitions is investigated. Sec. III focuses on homogeneous neutral two-flavor quark matter, the gapless 2SC (g2SC) phase and its properties are reviewed. In Sec. IV, a neutral mixed phase composed of the 2SC phase and normal quark matter is discussed. At last, a brief outlook is given in Sec. V.

B. Color superconducting phases

Let us start with the system of free fermion gas. Fermions obey the Pauli exclusion principle, which means no two identical fermions can occupy the same quantum state. The energy distribution for fermions (with mass m) has the form of

$$f(E_p) = \frac{1}{e^{\beta(E_p - \mu)} + 1}, \quad \beta = 1/T, \quad (1.1)$$

here $E_p = \sqrt{p^2 + m^2}$, μ is the chemical potential and T is the temperature. At zero temperature, $f(E_p) = \theta(\mu - E_p)$. The ground state of the free fermion gas is a filled Fermi sea, i.e., all states with the momenta less than the Fermi momentum $p_F = \sqrt{\mu^2 - m^2}$ are occupied, and the states with the momenta greater than the Fermi momentum p_F are empty. Adding or removing a single fermion costs no free energy at the Fermi surface.

For the degenerate Fermi gas, the only relevant fermion degrees of freedom are those near the Fermi surface. Considering two fermions near the Fermi surface, if there is a net

attraction between them, it turns out that they can form a bound state, i.e., Cooper pair [34]. The binding energy of the Cooper pair $\Delta(K)$ (K the total momentum of the pair), is very sensitive to K , being a maximum where $K = 0$. There is an infinite degeneracy among pairs of fermions with equal and opposite momenta at the Fermi surface. Because Cooper pairs are composite bosons, they will occupy the same lowest energy quantum state at zero temperature and produce a Bose-Einstein condensation. Thus the ground state of the Fermi system with a weak attractive interaction is a complicated coherent state of particle-particle Cooper pairs near the Fermi surface [24]. Exciting a quasiparticle and a hole which interact with the condensate requires at least the energy of 2Δ .

In QED case in condensed matter, the interaction between two electrons by exchanging a photon is repulsive. The attractive interaction to form electron-electron Cooper pairs is by exchanging a phonon, which is a collective excitation of the positive ion background. The Cooper pairing of the electrons breaks the electromagnetic gauge symmetry, and the photon obtains an effective mass. This indicates the Meissner effect [35], i.e., a superconductor expels the magnetic fields.

In QCD case at asymptotically high baryon density, the dominant interaction between two quarks is due to the one-gluon exchange. This naturally provides an attractive interaction between two quarks. The scattering amplitude for single-gluon exchange in an $SU(N_c)$ gauge theory is proportional to

$$(T_a)_{ki}(T_a)_{lj} = -\frac{N_c + 1}{4N_c}(\delta_{jk}\delta_{il} - \delta_{ik}\delta_{jl}) + \frac{N_c - 1}{4N_c}(\delta_{jk}\delta_{il} + \delta_{ik}\delta_{jl}). \quad (1.2)$$

Where T_a is the generator of the gauge group, and i, j and k, l are the fundamental colors of the two quarks in the incoming and outgoing channels, respectively. Under the exchange of the color indices of either the incoming or the outgoing quarks, the first term is antisymmetric, while the second term is symmetric. For $N_c = 3$, Eq. (1.2) represents that the tensor product of two fundamental colors decomposes into an (antisymmetric) color antitriplet and a (symmetric) color sextet,

$$[\mathbf{3}]^c \otimes [\mathbf{3}]^c = [\bar{\mathbf{3}}]^c_a \oplus [\mathbf{6}]^c_s. \quad (1.3)$$

In Eq. (1.2), the minus sign in front of the antisymmetric contribution indicates that the interaction in this antitriplet channel is attractive, while the interaction in the symmetric sextet channel is repulsive.

For cold dense quark matter, the attractive interaction in the color antitriplet channel induces the condensate of the quark-quark Cooper pairs, and the ground state is called the “color superconductivity”. Since the diquark cannot be color singlet, the diquark condensate breaks the local color $SU(3)_c$ symmetry, and the gauge bosons connected with the broken generators obtain masses. Comparing with the Higgs mechanism of dynamical gauge symmetry breaking in the Standard Model, here the diquark Cooper pair can be regarded as a composite Higgs particle. The calculation of the energy gap and the critical temperature from the first principles has been derived systematically in Refs. [36–43].

In reality, we are more interested in cold dense quark matter at moderate baryon density regime, i.e., $\mu_q \sim 500\text{MeV}$, which may exist in the interior of neutron stars. It is likely that cold dense quark droplet might be created in the laboratory through heavy ion collisions

in GSI-SPS energy scale. At these densities, an extrapolation of the asymptotic arguments becomes unreliable, we have to rely on effective models. Calculations in the framework of pointlike four-fermion interactions based on the instanton vertex [26,44–46], as well as in the Nambu–Jona-Lasinio (NJL) model [47–51] show that color superconductivity does occur at moderate densities, and the magnitude of diquark gap is around 100 MeV.

Even though the antisymmetry in the attractive channel signifies that only quarks with different colors can form Cooper pairs, color superconductivity has very rich phase structure because of its flavor, spin and other degrees of freedom. In the following, I list some of the known color superconducting phases.

The 2SC phase

Firstly we consider a system with only massless u and d quarks, assuming that the strange quark is much heavier than the up and down quarks. The color superconducting phase with only two flavors is normally called the 2SC phase.

Renormalization group arguments [36,52,53] suggest that possible quark pairs always condense in the s –wave. This means that the spin wave function of the pair is anti-symmetric. Since the diquark condenses in the color antitriplet $\bar{\mathbf{3}}_c$ channel, the color wave function of the pair is also anti-symmetric. The Pauli principle requires that the total wave function of the Cooper pair has to be antisymmetric under the exchange of the two quarks forming the pair. Thus the flavor wave function has to be anti-symmetric, too. This determines the structure of the order parameter

$$\Delta_{ij}^{\alpha\beta} = \Delta \epsilon_{ij} \epsilon^{\alpha\beta b}, \quad (1.4)$$

where color indices $\alpha, \beta \in (r, g, b)$ and flavor indices $i, j \in (u, d)$. From the order parameter Eq. (1.4), we can see that the condensate picks a color direction (here the *blue* direction, which is arbitrarily selected). The ground state is invariant under an $SU(2)_c$ subgroup of the color rotations that mixes the red and green colors, but the blue quarks are singled out as different. Thus the color $SU(3)_c$ is broken down to its subgroup $SU(2)_c$, and five of the gluons obtain masses, which indicates the Meissner effect [54].

In the 2SC phase, the Cooper pairs are $ud - du$ singlets and the global flavor symmetry $SU(2)_L \otimes SU(2)_R$ is intact, i.e., the chiral symmetry is not broken. There is also an unbroken global symmetry which plays the role of $U(1)_B$. Thus no global symmetry are broken in the 2SC phase.

The CFL phase

In the case when the chemical potential is much larger than the strange quark mass, we can assume $m_u = m_d = m_s = 0$, and there are three degenerate massless flavors in the system. The spin-0 order parameter should be color and flavor anti-symmetric, which has the form of

$$\Delta_{ij}^{\alpha\beta} = \Delta \sum_I \epsilon_{ijI} \epsilon^{\alpha\beta I}, \quad (1.5)$$

where color indices $\alpha, \beta \in (r, g, b)$ and flavor indices $i, j \in (u, d, s)$. Writing $\sum_I \epsilon_{ijI} \epsilon^{\alpha\beta I} = \delta_i^\alpha \delta_j^\beta - \delta_j^\alpha \delta_i^\beta$, we can see that the order parameter

$$\Delta_{ij}^{\alpha\beta} = \Delta(\delta_i^\alpha \delta_j^\beta - \delta_j^\alpha \delta_i^\beta) \quad (1.6)$$

describes the color-flavor locked (CFL) phase proposed in Ref. [55]. Many other different treatments [56–58] agreed that a condensate of the form (1.5) is the dominant condensate in three-flavor QCD.

In the CFL phase, all quark colors and flavors participate in the pairing. The color gauge group is completely broken, and all eight gluons become massive [55,59], which ensures that there are no infrared divergences associated with gluon propagators. Electromagnetism is no longer a separate symmetry, but corresponds to gauging one of the flavor generators. A rotated electromagnetism (“ \tilde{Q} ”) remains unbroken.

Two global symmetries, the chiral symmetry and the baryon number, are broken in the CFL phase, too. In zero-density QCD, the spontaneous breaking of chiral symmetry is due to the condensation of left-handed quarks with right-handed quarks. Here, at high baryon density, the chiral symmetry breaking occurs due to a rather different mechanism: locking of the flavor rotations to color. In the CFL phase, there is only pairing of left-handed quarks with left-handed quarks, and right-handed quarks with right-handed quarks, i.e.,

$$\langle \psi_{Li}^\alpha \psi_{Lj}^\beta \rangle = - \langle \psi_{Ri}^\alpha \psi_{Rj}^\beta \rangle. \quad (1.7)$$

Where L, R indicate left- and right-handed, respectively, α, β are color indices and i, j are flavor indices. A gauge invariant form [27,60,61]

$$\langle \psi_{Li}^\alpha \psi_{Lj}^\beta \bar{\psi}_{R\alpha}^k \bar{\psi}_{R\beta}^l \rangle \sim \langle \psi_{Li}^\alpha \psi_{Lj}^\beta \rangle \langle \bar{\psi}_{R\alpha}^k \bar{\psi}_{R\beta}^l \rangle \sim \Delta^2 \epsilon_{ijm} \epsilon^{klm} \quad (1.8)$$

captures the chiral symmetry breaking. The spectrum of excitations in the CFL phase contains an octet of Goldstone bosons associated with the chiral symmetry breaking. This looks remarkably like those at low density. In the excitation spectrum of the CFL phase, there is another singlet $U(1)$ Goldstone boson related to the baryon number symmetry breaking, which can be described using the order parameter

$$\langle udsuds \rangle \sim \langle \Lambda \Lambda \rangle. \quad (1.9)$$

In QCD with three degenerate light flavors, the spectrum in the CFL phase looks similar to that in the hyper-nuclear phase at low-density. It is suggested that the low density hyper-nuclear phase and the high density quark phase might be continuously connected [62].

Spin-1 color superconductivity

In the case of only one-flavor quark system, due to the antisymmetry in the color space, the Pauli principle requires that the Cooper pair has to occur in a symmetric spin channel. Therefore, in the simplest case, the Cooper pairs carry total spin one. Spin-1 color superconductivity was firstly studied in Ref. [25], for more recent and detailed discussions about the spin-1 gap, its critical temperature and Meissner effect, see Refs. [38,39,63–66]. For a review, see Ref. [67].

Pairing with mismatch: LOFF, CFL-K, g2SC and gCFL

To form the Cooper pair, the ideal case is when the two pairing quarks have the same Fermi momenta, i.e., $p_{F,i} = p_{F,j}$ with $p_{F,i} = \sqrt{\mu_{F,i}^2 - m_i^2}$, like in the ideal 2SC, CFL, and

spin-1 color superconducting phases. However, in reality, the nonzero strange quark mass or the requirement of charge neutrality induces a mismatch between the Fermi momenta of the two pairing quarks. When the mismatch is very small, it has little effect on the Cooper pairing. While if the mismatch is very large, the Cooper pair will be destroyed. The most interesting situation happens when the mismatch is neither very small nor very large.

LOFF: In the regime just on the edge of decoupling of the two pairing quarks (due to the nonzero strange quark mass for the qs Cooper pair with $q \in (u, d)$ or the chemical potential difference for the ud Cooper pair), a “LOFF” (Larkin-Ovchinnikov-Fulde-Ferrell) state may be formed. The LOFF state was firstly investigated in the context of electron superconductivity in the presence of magnetic impurities [68,69]. It was found that near the unpairing transition, it is favorable to form a state in which the Cooper pairs have nonzero momentum. This is favored because it gives rise to a regime of phase space where each of the two quarks in a pair can be close to its Fermi surface, and such pairs can be created at low cost in free energy. This sort of condensates spontaneously break translational and rotational invariance, leading to gaps which vary periodically in a crystalline pattern. The crystalline color superconductivity has been investigated in a series of papers, e.g., see Refs. [70–77].

CFL-K: The strange quark mass m_s induces an effective chemical potential $\mu_s = m_s^2/(2p_F)$, and the effects of the strange quark mass can be quite dramatic. In the CFL phase, the K^+ and K^0 modes may be unstable for large values of the strange quark mass to form a kaon condensation [78–81]. In the framework of effective theory [60,61,82–84], the masses of the Goldstone bosons can be determined as

$$\begin{aligned} m_{\pi^\pm} &= \mp \frac{m_d^2 - m_u^2}{2p_F} + \left[\frac{4A}{f_\pi^2} (m_u + m_d) m_s \right]^{1/2}, \\ m_{K^\pm} &= \mp \frac{m_s^2 - m_u^2}{2p_F} + \left[\frac{4A}{f_\pi^2} (m_u + m_s) m_d \right]^{1/2}, \\ m_{K^0, \bar{K}^0} &= \mp \frac{m_s^2 - m_d^2}{2p_F} + \left[\frac{4A}{f_\pi^2} (m_s + m_d) m_u \right]^{1/2}, \end{aligned} \tag{1.10}$$

with $A = 3\Delta^2/(4\pi^2)$ [61,85]. It was found that the kaon masses are substantially affected by the strange quark mass, the masses of K^- and \bar{K}^0 are pushed up while K^+ and K^0 are lowered. As a result, the K^+ and K^0 become massless if $m_s|_{crit} = 3.03 m_d^{1/3} \Delta^{2/3}$. For larger values of m_s the kaon modes are unstable, signaling the formation of a kaon condensate. For review of the kaon condensate in the CFL phase, see Ref. [31]. Recently, it was found that in the CFL phase, there also may exist η condensate [86].

g2SC and gCFL: When the β -equilibrium and the charge neutrality condition are required for the two-flavor quark system, the Fermi surfaces of the pairing u quark and d quark differ by μ_e , here μ_e is the chemical potential for electrons. It was found that when the gap parameter $\Delta < \mu_e/2$, the system will be in a new ground state called the gapless 2SC (g2SC) phase [87]. The g2SC phase has very unusual temperature properties [88] and chromomagnetic properties [89]. This phase will be introduced in more detail in Sec. III.

Similarly, for a charge neutral 3-flavor system with a nonzero strange quark mass m_s , with increasing m_s , the CFL phase transfers to a new gapless CFL (gCFL) phase when

$m_s^2/\mu \simeq 2\Delta$ [90]. The finite temperature property of the charge neutral three-flavor quark matter was investigated in Ref. [91–93]. Recently, it was shown that the kaon condensate shifts the critical strange quark mass to higher values for the appearance of the gCFL phase [94].

II. COMPETITION BETWEEN THE CHIRAL AND DIQUARK CONDENSATES

In this section, we are going to investigate the competition between the chiral and diquark condensates, and the content is based on Refs. [51,97].

In the idealized case at asymptotically high baryon densities, the color superconductivity with two massless flavors and the color-flavor-locking (CFL) phase with three degenerate massless quarks have been widely discussed from first principle QCD calculations. Usually, the diagrammatic methods are used at the asymptotic densities. The Green-function of the eight-component field and the gap equation were discussed in details in [38,95]. Neither current quark mass nor chiral condensate are necessary to be considered because they can be neglected compared to the very high Fermi surface. At less-than-asymptotic densities, the corrections of nonzero quark mass to the pure CFL phase can be treated perturbatively by expanding the current quark mass around the chiral limit [85,96].

For physical applications, we are more interested in the moderate baryon density regime, which may be related to the neutron stars and, in very optimistic cases even to heavy-ion collisions. To work out the phase structure from the hadron phase to the color superconducting phase, one should deal with the chiral condensate and the diquark condensate simultaneously. Because the chiral condensation contributes a dynamical quark mass, it is not reasonable any more to treat the quark mass term perturbatively in this density regime.

Usually, at moderate baryon density regime, effective models such as the instanton model, as well as the Nambu–Jona-Lasinio (NJL) model, are used. The model parameters are fixed in the QCD vacuum. In this regime, the usual way is to use the variational methods, which are enough for constructing the thermodynamic potential and the gap equation to investigate the ground state. In order to investigate the diquark excitations, and to calculate the cross-section of physical process in the color superconducting phase, it is very helpful to use the Green-function approach.

One of our main aims in this section is to apply the Green-function approach in the moderate baryon density regime. By using the energy projectors for massive quark, we can deal with the chiral and diquark condensates on an equal footing, and we will deduce the Nambu-Gorkov massive quark propagator [97] as well as the thermodynamic potential [51].

In the normal phase, the quarks of different colors are degenerate. While in the color broken phase, it is natural to assume that the quarks involved in the diquark condensate are different from the free quarks. It is difficult to obtain the mass expression for the quarks participating in the diquark condensate, because the particles and holes mix with each other, and the elementary excitations are quasi-particles and quasi-holes near the Fermi surface. The difference between quarks in different colors has been reflected by their propagators, and the difference can be read through calculating the quarks chiral condensate. In the chiral limit, the chiral condensate disappears entirely in the color superconducting phase, and it is not possible to investigate the influence of the color breaking on quarks in different

colors, so we keep the small current quark mass in this section.

In the moderate baryon density regime, people are interested in whether there exists a regime where both the chiral symmetry and color symmetry are broken [45–47, 98–102]. Note that the presence of a small current quark mass induces that the chiral symmetry only restores partially and there always exists a small chiral condensate in the color superconducting phase. This phenomenon had been called coexistence of the chiral and diquark condensates in Ref. [45]. In the coexistence regime resulted by current quark mass, the chiral condensate is small comparing with the diquark condensate, and the role of the chiral condensate can be prescribed by the Anderson theorem [102], i.e., in this phase, the contribution of the chiral condensate to thermodynamic quantities becomes strongly suppressed, and one can calculate the diquark condensate neglecting the influence of the chiral condensate.

In order to differ from the coexistence of the diquark condensate and the small chiral condensate in the chiral symmetry restoration phase, the coexistence of the diquark condensate and the dynamical chiral condensate in the chiral symmetry breaking phase is called the *double broken phase*. The existence of the double broken phase depends on the coupling constants G_S and G_D in the quark-antiquark and diquark channels [47, 101]. In the case of small ratio of $G_D/G_S < 1$, the calculations in the instanton model [45], NJL model [47] and random matrix model [101] show that there is no double broken phase. While for $G_D/G_S > 1$ the calculations in the the random matrix model [101] and the NJL model [47] show that there exists a narrow regime where both chiral (dynamical) symmetry and color symmetry are broken, and the chiral and diquark condensate coexist. The larger value of G_D/G_S is, the wider regime of the double broken phase has been found in the random matrix model [101].

In this section, based on Ref. [51], we explain the existence of the double broken phase by analyzing the influence of the diquark condensate on the Fermi surface of the constituent quark. In the mean-field approximation of the NJL model, the thermal system of the constituent quarks is nearly an ideal Fermi gas, and there is a sharp Fermi surface for the constituent quark. When a diquark condensate is formed, the Cooper pair smoothes the Fermi surface, and this induces the chiral symmetry restoring at a smaller chemical potential. The stronger the coupling constant in the diquark channel, the larger the diquark gap will be, and the smaller critical chemical potential will be for the color superconductivity phase transition. However, it is found in Ref. [51] that, if $G_D/G_S > 1$, the diquark condensate starts to appear even in the vacuum. This may suggest that in the NJL model, the diquark coupling strength G_D should not be larger than the quark-antiquark coupling strength G_S . It is also possible that the appearance of the diquark condensate in vacuum is an artificial result due to the lack of deconfinement in the NJL model.

A. The extended NJL model

To describe quark matter in the intermediate baryon density regime, we use the extended NJL model. The choice of the NJL model [103] is motivated by the fact that this model displays the same symmetries as QCD and that it describes well the spontaneous breakdown of chiral symmetry in the vacuum and its restoration at high temperature and density. For the review of the NJL model, please see [104]. The model we used in this paper is an

extended version of the two-flavor NJL model including interactions in the color singlet quark-antiquark channel as well as in the color anti-triplet diquark channel, which is not directly extended from the NJL model, but from the QCD Lagrangian [105–107].

The importance of color $\bar{3}$ diquark degree of freedom is related to the fact that one can construct a color-singlet nucleon current based on it. Because the gluon exchange between two quarks in the color $\bar{3}$ channel is attractive, one can view a color singlet baryon as a quark-diquark bound state. And experimental data from ep collisions indicate the existence of this quark-diquark component in nucleons [108]. The discovery of the pentaquark also reminds us the importance of the diquark degree of freedom [6,7,109].

The first attempt to investigate the diquark properties in the NJL model was taken in Ref. [110]. Starting from an NJL model for scalar, pseudoscalar, vector and axial-vector interactions of the $(\bar{q}q) \times (\bar{q}q)$ type and Fierz-transforming away the vector and axial-vector interactions, the scalar and pseudoscalar mesons, and diquarks can be obtained. However, this method could not get a consistent treatment of vector and axial-vector particles.

The extended NJL model we use is derived from the QCD Lagrangian [105,106]. Integrating out the gluon degrees of freedom from the QCD Lagrangian, and performing a local approximation for the (nonperturbative) gluon propagator, one obtains a contact current-current interaction. By using a special Fierz-rearrangement [111] (see Appendix A), one can completely decompose the two-quark-current interaction term into “attractive” color singlet $(\bar{q}q)$ and color antitriplet (qq) channels. In this way, a complete simultaneous description of scalar, pseudo-scalar, vector, and axial-vector mesons and diquarks is possible, thus the extended NJL model including $(\bar{q}q) \times (\bar{q}q)$ interactions is completed by a corresponding $(\bar{q}\bar{q}) \times (qq)$ interaction part.

It is worth to mention that, in the mean-field approximation, there is a famous ambiguity connected with performing the Fierz transformation for the pointlike four-fermion interaction. For more detail discussion about the Fierz ambiguity, see Ref. [113]. Here, in this paper, we only consider the scalar, pseudoscalar mesons and scalar diquark, and the Lagrangian density has the form

$$\mathcal{L} = \bar{q}(i\gamma^\mu\partial_\mu - m_0)q + G_S[(\bar{q}q)^2 + (\bar{q}i\gamma_5\tau q)^2] + G_D[(i\bar{q}^C\varepsilon\epsilon^b\gamma_5q)(i\bar{q}\varepsilon\epsilon^b\gamma_5q^C)]. \quad (2.1)$$

Where $q^C = C\bar{q}^T$, $\bar{q}^C = q^TC$ are charge-conjugate spinors, $C = i\gamma^2\gamma^0$ is the charge conjugation matrix (the superscript T denotes the transposition operation). For more details about the charge conjugate, see Appendix B. m_0 is the current quark mass, the quark field $q \equiv q_{i\alpha}$ with $i = 1, 2$ and $\alpha = 1, 2, 3$ is a flavor doublet and color triplet, as well as a four-component Dirac spinor, $\tau = (\tau^1, \tau^2, \tau^3)$ are Pauli matrices in the flavor space, where τ^2 is antisymmetric, and $(\varepsilon)^{ik} \equiv \varepsilon^{ik}$, $(\epsilon^b)^{\alpha\beta} \equiv \epsilon^{\alpha\beta b}$ are totally antisymmetric tensors in the flavor and color spaces.

Though, from the Fierz transformation, the quark-antiquark coupling constant G_S and the diquark coupling constant G_D have the relation $G_D = G_S N_c/(2N_c - 2)$, in this article, G_S and G_D are treated independently. The former is responsible for the meson excitations, and the latter for the diquark excitations, which in principle can be determined by fitting meson and baryon properties in the vacuum. In Ref. [106], the ratio of coupling constants $G_D/G_S \simeq 2.26/3$ was obtained by fitting the scalar diquark mass of 600 MeV to get a realistic vacuum baryon mass. It is noticed that this ratio is quite close to the value 3/4 obtained from Fierz transformation.

The attractive interaction in different channels in the Lagrangian gives rise to a very rich structure of the phase diagram. At zero temperature and density, the attractive interaction in the color singlet channel is responsible for the appearance of a quark-antiquark condensate and for the spontaneous breakdown of the chiral symmetry, and the interaction in the qq channel binds quarks into diquarks (and baryons), but is not strong enough to induce diquark condensation. As the density increases, Pauli blocking suppresses the $\bar{q}q$ interaction, while the attractive interaction in the color anti-triplet diquark channel will induce the quark-quark condensate around the Fermi surface which can be identified as a superconducting phase.

After bosonization [105,106,112], one obtains the linearized version of the model, i.e., in the mean-field approximation,

$$\begin{aligned}\tilde{\mathcal{L}} = & \bar{q}(i\gamma^\mu\partial_\mu - m_0)q - \bar{q}(\sigma + i\gamma^5\tau\pi)q - \frac{1}{2}\Delta^{*b}(i\bar{q}^C\varepsilon\epsilon^b\gamma_5q) - \frac{1}{2}\Delta^b(i\bar{q}\varepsilon\epsilon^b\gamma_5q^C) \\ & - \frac{\sigma^2 + \pi^2}{4G_S} - \frac{\Delta^{*b}\Delta^b}{4G_D},\end{aligned}\quad (2.2)$$

with the bosonic fields

$$\Delta^b \sim i\bar{q}^C\varepsilon\epsilon^b\gamma_5q, \quad \Delta^{*b} \sim i\bar{q}\varepsilon\epsilon^b\gamma_5q^C, \quad \sigma \sim \bar{q}q, \quad \pi \sim i\bar{q}\gamma^5\tau q. \quad (2.3)$$

Clearly, the σ and π fields are color singlets, and the diquark fields Δ^b and Δ^{*b} are color antitriplet and (isoscalar) singlet under the chiral $SU(2)_L \times SU(2)_R$ group. $\sigma \neq 0$ and $\Delta^b \neq 0$ indicate that the chiral symmetry and the color symmetry are spontaneously broken. Here it has been regarded that only the red and green quarks participating in the condensate, while the blue quarks do not. The real ground state at any T, μ will be determined by the minimum of the thermodynamic potential.

The partition function of the grand canonical ensemble can be evaluated by using the standard method [114,115],

$$\mathcal{Z} = N' \int [d\bar{q}][dq] \exp \left\{ \int_0^\beta d\tau \int d^3\mathbf{x} (\tilde{\mathcal{L}} + \mu\bar{q}\gamma_0q) \right\}, \quad (2.4)$$

where μ is the chemical potential, and $\beta = 1/T$ is the inverse of the temperature T .

In the mean field approximation, we can write the partition function as a product of three parts,

$$\mathcal{Z} = \mathcal{Z}_{const}\mathcal{Z}_b\mathcal{Z}_{r,g}. \quad (2.5)$$

The constant part is

$$\mathcal{Z}_{const} = N' \exp \left\{ - \int_0^\beta d\tau \int d^3\mathbf{x} \left[\frac{\sigma^2}{4G_S} + \frac{\Delta^*\Delta}{4G_D} \right] \right\}. \quad (2.6)$$

The contribution from free blue quarks has the form

$$\begin{aligned}\mathcal{Z}_b = & \int [d\bar{q}_b][dq_b] \exp \left\{ \int_0^\beta d\tau \int d^3\mathbf{x} \left[\frac{1}{2}\bar{q}_b(i\gamma^\mu\partial_\mu - m + \mu\gamma_0)q_b \right. \right. \\ & \left. \left. + \frac{1}{2}\bar{q}_b^C(i\gamma^\mu\partial_\mu - m - \mu\gamma_0)q_b^C \right] \right\}.\end{aligned}\quad (2.7)$$

For the quarks with red and green color $Q = q_{r,g}$ participating in the quark condensate, their contribution is

$$\mathcal{Z}_{r,g} = \int [d\bar{Q}][dQ] \exp \left\{ \int_0^\beta d\tau \int d^3\mathbf{x} \left[\frac{1}{2} \bar{Q} (i\gamma^\mu \partial_\mu - m + \mu\gamma_0) Q + \frac{1}{2} \bar{Q}^C (i\gamma^\mu \partial_\mu - m - \mu\gamma_0) Q^C + \frac{1}{2} \bar{Q} \Delta^- Q^C + \frac{1}{2} \bar{Q}^C \Delta^+ Q \right] \right\}. \quad (2.8)$$

Here we have introduced the constituent quark mass

$$m = m_0 + \sigma, \quad (2.9)$$

and defined Δ^\pm as

$$\Delta^- = -i\Delta\varepsilon\epsilon^b\gamma_5, \quad \Delta^+ = -i\Delta^*\varepsilon\epsilon^b\gamma_5 \quad (2.10)$$

with the relation $\Delta^+ = \gamma^0(\Delta^-)^\dagger\gamma^0$.

B. Nambu-Gorkov propagator with chiral and diquark condensates

In the case of finite chemical potential, it is more convenient to use the Nambu-Gorkov formalism. Introducing the 8-component spinors for the blue quarks and the quarks colored with red and green, respectively

$$\Psi_b = \begin{pmatrix} q_b \\ q_b^C \end{pmatrix}, \quad \bar{\Psi}_b = (\bar{q}_b \quad \bar{q}_b^C), \quad (2.11)$$

$$\Psi = \begin{pmatrix} Q \\ Q^C \end{pmatrix}, \quad \bar{\Psi} = (\bar{Q} \quad \bar{Q}^C), \quad (2.12)$$

and using the Fourier transformation in the momentum space,

$$q(x) = \frac{1}{\sqrt{V}} \sum_n \sum_{\mathbf{p}} e^{-i(\omega_n \tau - \mathbf{p} \cdot \mathbf{x})} q(\mathbf{p}), \quad (2.13)$$

where V is the volume of the thermal system, we can re-write the partition function Eqs. (2.7) and (2.8) in the momentum space as

$$\begin{aligned} \mathcal{Z}_b &= \int [d\Psi_b] \exp \left\{ \frac{1}{2} \sum_{n,\mathbf{p}} \bar{\Psi}_b \frac{G_0^{-1}}{T} \Psi_b \right\} \\ &= \text{Det}^{1/2}(\beta G_0^{-1}), \end{aligned} \quad (2.14)$$

and

$$\begin{aligned} \mathcal{Z}_{r,g} &= \int [d\Psi] \exp \left\{ \frac{1}{2} \sum_{n,\mathbf{p}} \bar{\Psi} \frac{G^{-1}}{T} \Psi \right\} \\ &= \text{Det}^{1/2}(\beta G^{-1}). \end{aligned} \quad (2.15)$$

Where the determinantal operation Det is to be carried out over the Dirac, color, flavor and the momentum-frequency space. In Eqs. (2.14) and (2.15), we have defined the quark propagator in the normal phase

$$G_0^{-1} = \begin{pmatrix} [G_0^+]^{-1} & 0 \\ 0 & [G_0^-]^{-1} \end{pmatrix}, \quad (2.16)$$

with

$$[G_0^\pm]^{-1} = (p_0 \pm \mu) \gamma_0 - \boldsymbol{\gamma} \cdot \mathbf{p} - m \quad (2.17)$$

and the quark propagator in the color broken phase

$$G^{-1} = \begin{pmatrix} [G_0^+]^{-1} & \Delta^- \\ \Delta^+ & [G_0^-]^{-1} \end{pmatrix}. \quad (2.18)$$

The Nambu-Gorkov propagator $G(P)$ is determined from solving $1 = G^{-1} G$,

$$G = \begin{pmatrix} G^+ & \Xi^- \\ \Xi^+ & G^- \end{pmatrix}, \quad (2.19)$$

with the components

$$G^\pm \equiv \left\{ [G_0^\pm]^{-1} - \Sigma^\pm \right\}^{-1}, \quad \Sigma^\pm \equiv \Delta^\mp G_0^\mp \Delta^\pm, \\ \Xi^\pm \equiv -G^\mp \Delta^\pm G_0^\pm = -G_0^\mp \Delta^\pm G^\pm. \quad (2.20)$$

Here all components depend on the 4-momentum P .

In the case of the mass term $m = 0$, the Nambu-Gorkov quark propagator has a simple form which could be derived from the energy projectors for massless particles [38,95]. If there is a small mass term, the quark propagator can be expanded perturbatively around $m = 0$, but the form is very complicated [96]. In our case the quark mass term cannot be treated perturbatively, we have to find a general way to deal with the massive quark propagator.

Fortunately, we can evaluate a simple form for the massive quark propagator by using the energy projectors for massive particles. The energy projectors onto states of positive and negative energy for free massive particles are defined as

$$\Lambda_\pm(\mathbf{p}) = \frac{1}{2} \left(1 \pm \frac{\gamma_0(\boldsymbol{\gamma} \cdot \mathbf{p} + m)}{E_p} \right), \quad (2.21)$$

where the quark energy $E_p = \sqrt{\mathbf{p}^2 + m^2}$. Under the transformation of γ_0 and γ_5 , we can get another two energy projectors $\tilde{\Lambda}_\pm$,

$$\tilde{\Lambda}_\pm(\mathbf{p}) = \frac{1}{2} \left(1 \pm \frac{\gamma_0(\boldsymbol{\gamma} \cdot \mathbf{p} - m)}{E_p} \right), \quad (2.22)$$

which satisfy

$$\gamma_0 \Lambda_{\pm}(\mathbf{p}) \gamma_0 = \tilde{\Lambda}_{\mp}(\mathbf{p}), \quad \gamma_5 \Lambda_{\pm}(\mathbf{p}) \gamma_5 = \tilde{\Lambda}_{\pm}(\mathbf{p}). \quad (2.23)$$

The normal quark propagator elements can be re-written as

$$G_0^{\pm} = \frac{\gamma_0 \tilde{\Lambda}_+}{p_0 + E_p^{\pm}} + \frac{\gamma_0 \tilde{\Lambda}_-}{p_0 - E_p^{\mp}}, \quad (2.24)$$

with $E_p^{\pm} = E_p \pm \mu$. The propagator has four poles, i.e.,

$$p_0 = \pm E_p^-, \quad p_0 = \mp E_p^+, \quad (2.25)$$

where the former two correspond to the excitation energies of particles and holes, and the latter two are for antiparticles and antiholes, respectively.

The full quark propagator G , i.e., (2.19) can be evaluated [97]. The normal quark propagator has the form

$$G^{\pm} = \left(\frac{p_0 - E_p^{\pm}}{p_0^2 - E_{\Delta}^{\pm 2}} \gamma_0 \tilde{\Lambda}_+ + \frac{p_0 + E_p^{\mp}}{p_0^2 - E_{\Delta}^{\mp 2}} \gamma_0 \tilde{\Lambda}_- \right) (\delta_{\alpha\beta} - \delta_{\alpha b} \delta_{\beta b}) \delta^{ij}, \quad (2.26)$$

and the abnormal quark propagator reads

$$\Xi^{\pm} = \left(\frac{\Delta^{\pm}}{p_0^2 - E_{\Delta}^{\pm 2}} \tilde{\Lambda}_+ + \frac{\Delta^{\pm}}{p_0^2 - E_{\Delta}^{\mp 2}} \tilde{\Lambda}_- \right), \quad (2.27)$$

with $E_{\Delta}^{\pm 2} = E_p^{\pm 2} + \Delta^2$. This propagator is similar to the massless propagator derived in [95].

The four poles of the Nambu-Gorkov propagator, i.e.,

$$p_0 = \pm E_{\Delta}^-, \quad p_0 = \mp E_{\Delta}^+, \quad (2.28)$$

correspond to the excitation energies of quasi-particles (quasi-holes) and quasi-antiparticle (quasi-antiholes) in the color broken phase. These quasi-particles are superpositions of particles and holes, and are called “Bogoliubons”. In the normal phase, exciting a pair of a particle and a hole on the Fermi surface does not need energy, while in the superconducting phase, exciting a quasi-particle and a hole needs at least the energy 2Δ at $E_p = \mu$.

C. Gap equations

With the Nambu-Gorkov quark propagator Eqs. (2.26) and (2.27), one can investigate the meson excitations [116], and physical processes related to the transport properties. The chiral and diquark condensates can also be generally expressed from the quasi-particle propagator. The diquark condensate has the form

$$\langle \bar{q}^C \gamma_5 q \rangle = -iT \sum_n \int \frac{d^3 \mathbf{p}}{(2\pi)^3} \text{tr}[\Xi^- \gamma_5]. \quad (2.29)$$

From general consideration, there should be eight Dirac components of the diquark condensates [25,95,117,118]. In the case of the NJL type model, the diquark condensates related to momentum vanish, and there is only one independent 0^+ diquark gap with Dirac structure $\Gamma = \gamma_5$ for massless quark, and there exists another 0^+ diquark condensate with Dirac structure $\Gamma = \gamma_0\gamma_5$ at nonzero quark mass. In this paper, we assume the contribution of the diquark condensate with $\Gamma = \gamma_0\gamma_5$ is small, and only consider the diquark condensate with $\Gamma = \gamma_5$.

Performing the Matsubara frequency summation and taking the limit $T \rightarrow 0$, we get the diquark condensate at finite chemical potential

$$\langle \bar{q}^C \gamma_5 q \rangle = -2\Delta N_c N_f \int \frac{d^3 \mathbf{p}}{(2\pi)^3} \left[\frac{1}{2E_\Delta^-} + \frac{1}{2E_\Delta^+} \right]. \quad (2.30)$$

Using the relation between the diquark gap Δ and the diquark condensate $\langle \bar{q}^C \gamma_5 q \rangle$, i.e.,

$$\Delta = -2G_D \langle \bar{q}^C \gamma_5 q \rangle, \quad (2.31)$$

the gap equation for the diquark condensate in the limit of $T \rightarrow 0$ can be written as

$$1 = 8N_f G_D \int \frac{d^3 \mathbf{p}}{(2\pi)^3} \left[\frac{1}{2E_\Delta^-} + \frac{1}{2E_\Delta^+} \right]. \quad (2.32)$$

The quark mass has the expression

$$\begin{aligned} m &= m_0 - 2G_S \langle \bar{q}q \rangle, \\ \langle \bar{q}q \rangle &= 2 \langle \bar{q}_r q_r \rangle + \langle \bar{q}_b q_b \rangle. \end{aligned} \quad (2.33)$$

Where the chiral condensate for the free blue quarks is

$$\langle \bar{q}_b q_b \rangle = -iT \sum_n \int \frac{d^3 \mathbf{p}}{(2\pi)^3} \text{tr}[G_0^+], \quad (2.34)$$

and the chiral condensate for the red and green quarks reads

$$\langle \bar{q}_r q_r \rangle = -iT \sum_n \int \frac{d^3 \mathbf{p}}{(2\pi)^3} \text{tr}[G^+]. \quad (2.35)$$

In the limit $T \rightarrow 0$, the gap equation for the quark mass has the form

$$m = m_0 - 8mN_f G_S \int \frac{d^3 \mathbf{p}}{(2\pi)^3} \frac{1}{2E_p} [\theta(\mu - E_p) - 1 + 2(n_p^+ - n_p^-)]. \quad (2.36)$$

Where

$$n_p^\pm = \frac{1}{2} \left(1 \mp \frac{E_p^\mp}{E_\Delta^\mp} \right) \quad (2.37)$$

are the occupation numbers for quasi-particles and quasi-antiparticles at $T = 0$. Correspondingly, $1 - n_p^\pm$ are the occupation numbers of quasi-holes and quasi-antiholes, respectively.

The difference between the quarks participating in the diquark condensate and the free blue quark can be read from their chiral condensates,

$$\delta = \langle \bar{q}_b q_b \rangle^{1/3} - \langle \bar{q}_r q_r \rangle^{1/3}, \quad (2.38)$$

where δ has the dimension of energy. In the case of chiral limit, the quark mass m decreases to zero in the color superconducting phase, and the influence of the diquark condensate on quarks in different colors vanishes.

D. Derivation of the thermodynamic potential

Now let us derive the thermodynamic potential. For the blue quarks which do not participate in the diquark condensate, from Eq. (2.14), we have

$$\ln \mathcal{Z}_{q_b} = \frac{1}{2} \ln \{ \text{Det}(\beta[G_0]^{-1}) = \frac{1}{2} \ln [\text{Det}(\beta[G_0^+]^{-1}) \text{Det}(\beta[G_0^-]^{-1})]. \quad (2.39)$$

Using the Dirac matrix, we first perform the determinant in the Dirac space,

$$\begin{aligned} \text{Det} \beta [G_0^+]^{-1} &= \text{Det} \beta [(p_0 + \mu) \gamma_0 - \boldsymbol{\gamma} \cdot \mathbf{p} - m] \\ &= \text{Det} \beta \begin{pmatrix} (p_0 + \mu) - m & \boldsymbol{\sigma} \cdot \mathbf{p} \\ -\boldsymbol{\sigma} \cdot \mathbf{p} & -(p_0 + \mu) - m \end{pmatrix}, \\ &= -\beta^2 [(p_0 + \mu)^2 - E_p^2], \end{aligned} \quad (2.40)$$

and in a similar way, we get

$$\text{Det} \beta [G_0^-]^{-1} = -\beta^2 [(p_0 - \mu)^2 - E_p^2]. \quad (2.41)$$

After performing the determinant in the Dirac space, we have

$$\text{Det} \beta [G_0^+]^{-1} \text{Det} \beta [G_0^-]^{-1} = \beta^2 [p_0^2 - (E_p + \mu)^2] \beta^2 [p_0^2 - (E_p - \mu)^2]. \quad (2.42)$$

Considering the determinant in the flavor, color, spin spaces and momentum-frequency space, we get the standard expression

$$\ln \mathcal{Z}_{q_b} = N_f \sum_n \sum_{\mathbf{p}} \{ \ln(\beta^2 [p_0^2 - (E_p + \mu)^2]) + \ln(\beta^2 [p_0^2 - (E_p - \mu)^2]) \}, \quad (2.43)$$

remembering that the color space for the blue quark is one-dimensional.

It is more complicated to evaluate the thermodynamic potential for the quarks participating in the diquark condensate. From Eq. (2.15), we have

$$\ln \mathcal{Z}_{q_r, g} = \frac{1}{2} \ln \text{Det}(\beta G^{-1}). \quad (2.44)$$

For a 2×2 matrix with elements A, B, C and D , we have the identity

$$\text{Det} \begin{pmatrix} A & B \\ C & D \end{pmatrix} = \text{Det}(-CB + CAC^{-1}D) == \text{Det}(-BC + BDB^{-1}A). \quad (2.45)$$

Replacing A, B, C and D with the corresponding elements of G^{-1} , we have

$$\begin{aligned}\text{Det}(\beta G^{-1}) &= \beta^2 \text{Det}D_1 = \beta^2 \text{Det}[-\Delta^+ \Delta^- + \Delta^+ [G_0^+]^{-1} [\Delta^+]^{-1} [G_0^-]^{-1}] \\ &= \beta^2 \text{Det}D_2 = \beta^2 \text{Det}[-\Delta^+ \Delta^- + [G_0^-]^{-1} [\Delta^-]^{-1} [G_0^+]^{-1} \Delta^-].\end{aligned}\quad (2.46)$$

Using the energy projectors $\tilde{\Lambda}_\pm$, we can work out D_1 and D_2 as

$$\begin{aligned}D_1 &= \Delta^2 + \gamma_5 [\gamma_0(p_0 - E_p^-) \Lambda_+ + \gamma_0(p_0 + E_p^+) \Lambda_-] \gamma_5 [\gamma_0(p_0 - E_p^+) \Lambda_+ + \gamma_0(p_0 + E_p^-) \Lambda_-] \\ &= -[(p_0^2 - E_p^{-2} - \Delta^2) \Lambda_- + (p_0^2 - E_p^{+2} - \Delta^2) \Lambda_+], \\ D_2 &= -[(p_0^2 - E_p^{-2} - \Delta^2) \Lambda_+ + (p_0^2 - E_p^{+2} - \Delta^2) \Lambda_-].\end{aligned}\quad (2.47)$$

Using the properties of the energy projectors, one can get

$$D_1 D_2 = [p_0^2 - E_\Delta^{-2}] [p_0^2 - E_\Delta^{+2}]. \quad (2.48)$$

With the above equations, Eq. (2.44) can be expressed as

$$\begin{aligned}\ln \mathcal{Z}_{q_{r,g}} &= \frac{1}{2} \ln [\text{Det} \beta G^{-1}] = \frac{1}{4} \text{Trln} [\beta^2 D_1 \beta^2 D_2] \\ &= \frac{1}{4} \{ \text{Trln} [\beta^2 (p_0^2 - E_\Delta^{-2})] + \text{Trln} [\beta^2 (p_0^2 - E_\Delta^{+2})] \} \\ &= 2N_f \sum_n \sum_p \{ \ln [\beta^2 (p_0^2 - E_\Delta^{-2})] + \ln [\beta^2 (p_0^2 - E_\Delta^{+2})] \}.\end{aligned}\quad (2.49)$$

The frequency summation of the free-energy

$$\ln \mathcal{Z}_f = \sum_n \ln [\beta^2 (p_0^2 - E_p^2)] \quad (2.50)$$

can always be obtained by performing the frequency summation of the propagator $1/(p_0^2 - E_p^2)$. Differentiate Eq. (2.50) with respect to E_p :

$$\frac{\partial \ln \mathcal{Z}_f}{\partial E_p} = -2E_p \sum_n \frac{1}{p_0^2 - E_p^2} = \beta [1 - 2\tilde{f}(E_p)], \quad (2.51)$$

where $\tilde{f}(x) = 1/(e^{\beta x} + 1)$ is the usual Fermi-Dirac distribution function. Then integrating with respect to E_p , one can get the free-energy

$$\ln \mathcal{Z}_f = \beta [E_p + 2T \ln(1 + e^{-\beta E_p})]. \quad (2.52)$$

With the help of the above expression, and replacing

$$\sum_p \rightarrow V \int \frac{d^3 \mathbf{p}}{(2\pi)^3}, \quad (2.53)$$

one can have

$$\begin{aligned}\ln \mathcal{Z}_{qb} &= N_f \beta V \int \frac{d^3 p}{(2\pi)^3} [E_p^+ + 2T \ln(1 + e^{-\beta E_p^+}) + E_p^- + 2T \ln(1 + e^{-\beta E_p^-})], \\ \ln \mathcal{Z}_{qr,g} &= 2N_f \beta V \int \frac{d^3 p}{(2\pi)^3} [E_\Delta^+ + 2T \ln(1 + e^{-\beta E_\Delta^+}) + E_\Delta^- + 2T \ln(1 + e^{-\beta E_\Delta^-})].\end{aligned}\quad (2.54)$$

Finally, we obtain the familiar expression of the thermodynamic potential

$$\begin{aligned}\Omega = -T \frac{\ln Z}{V} &= \frac{\sigma^2}{4G_S} + \frac{\Delta^2}{4G_D} - 2N_f \int \frac{d^3 p}{(2\pi)^3} [E_p + T \ln(1 + e^{-\beta E_p^+}) + T \ln(1 + e^{-\beta E_p^-}) \\ &+ E_\Delta^+ + 2T \ln(1 + e^{-\beta E_\Delta^+}) + E_\Delta^- + 2T \ln(1 + e^{-\beta E_\Delta^-})].\end{aligned}\quad (2.55)$$

The two gap equations Δ and m in Eqs. (2.32) and (2.36) can be equivalently derived by minimizing the thermodynamic potential Eq. (2.55) with respect to m and Δ , respectively, i.e.,

$$\frac{\partial \Omega}{\partial \Delta} = 0, \quad \frac{\partial \Omega}{\partial m} = 0. \quad (2.56)$$

E. Competition between the chiral and diquark condensates

In this subsection, through numerical calculations, we will investigate the phase structure along the chemical potential direction, analyze the competition mechanism between the chiral condensate and diquark condensate, and discuss the influence of the color breaking on the quarks with different colors.

Before the numerical calculations, we should fix the model parameters. The current quark mass $m_0 = 5.5\text{MeV}$, the Fermion momentum cut-off $\Lambda_f = 0.637\text{GeV}$, and the coupling constant in color singlet channel $G_S = 5.32\text{GeV}^{-2}$ are determined by fitting vacuum properties. The corresponding constituent quark mass in the vacuum is taken to be $m(\mu = 0) = 330\text{MeV}$. The coupling constant in the color anti-triplet channel G_D can in principle be determined by fitting the nucleon properties, here, we choose G_D/G_S as a free parameter.

The double broken phase

Firstly, we investigate the phase structure along the chemical potential direction with respect to different magnitude of G_D/G_S . In the explicit chiral symmetry breaking case, we define the point at which the chiral condensate has maximum change as the critical chemical potential μ_χ for the chiral phase transition, and the point at which the diquark condensate starts to appear as the critical chemical potential μ_Δ for the color superconductivity phase transition. The two gaps m (white points) and Δ (black points) determined by Eqs. (2.32) and (2.36) are plotted in Fig. 1 as functions of μ with respect to different $G_D/G_S = 2/3, 1, 1.2, 1.5$ in (a), (b), (c) and (d), respectively.

In Fig. 1 (a), i.e., in the case of $G_D/G_S = 2/3$, we see that the chiral phase transition and the color superconductivity phase transition occur nearly at the same chemical potential $\mu_\chi \simeq \mu_\Delta = 340 \text{ MeV}$. The two phase transitions are of first order. In the explicit chiral symmetry breaking case, there is a small chiral condensate in the color superconductivity

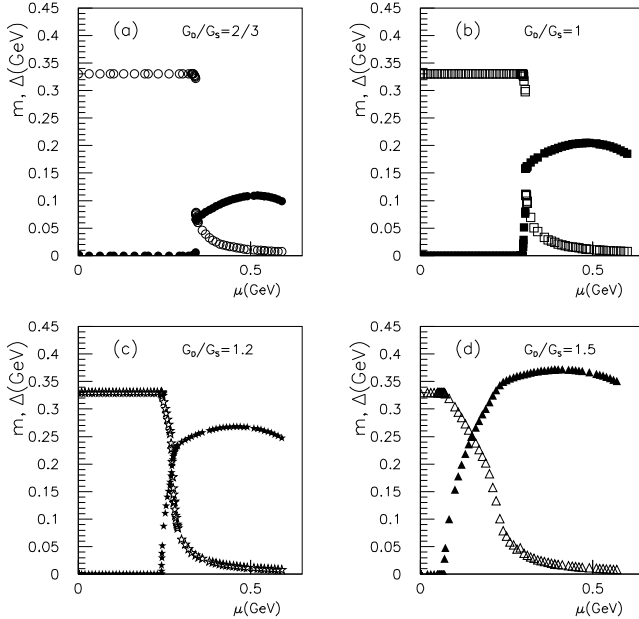


FIG. 1. The two gaps m (white points) and Δ (black points) as functions of chemical potential μ for $G_D/G_S = 2/3, 1, 1.2, 1.5$, respectively.

phase $\mu > \mu_\chi$. This phenomena has been called the coexistence of the chiral and diquark condensate in Ref. [45]. In this coexistence regime, the chiral condensate is small and can be described by the Anderson theorem [102].

In Fig. 1 (b), with $G_D/G_S = 1$, the diquark condensate starts to appear at $\mu_\Delta = 298$ MeV, and the chiral symmetry restores at $\mu_\chi = 304.8$ MeV. Both μ_Δ and μ_χ are smaller than those in the case of $G_D/G_S = 2/3$. In the regime from μ_Δ to μ_χ , we also see the coexistence of the chiral and diquark condensates. However, the chiral condensate in this regime is not due to the explicit symmetry breaking but due to the dynamical symmetry breaking. In order to differ the coexistence of the diquark condensate and the small quark-antiquark condensate in the chiral symmetric phase as in Fig. 1 (a), we call the coexistence of the diquark condensate and the large quark-antiquark condensate in the chiral symmetry broken phase as the “double broken phase”. The diquark gap increases continuously from zero to 82 MeV in this double broken phase, and jumps up to 152 MeV at the critical point μ_χ .

In Fig. 1 (c) and (d), we see that with increasing of G_D/G_S , the diquark condensate starts to appear at smaller μ_Δ , and chiral symmetry restores at smaller μ_χ , while the width of the regime of double broken phase, $\mu_\chi - \mu_\Delta$, becomes larger. This phenomena has also been found in Ref. [101] in the random matrix model.

However, as shown in Fig. 2 (b), (c) and (d), in the three cases $G_D/G_S = 1, 1.2, 1.5$, the diquark condensate starts to appear even in the vacuum where $n_b = 0$ with n_b the baryon

number density. This, of course, is not physical, because a nonzero diquark condensate means the appearance of a nonzero Majorana mass for quarks in vacuum. This would be in conflict with the standard definition of the bayron number in vacuum. The appearance of the diquark condensate in the vacuum may indicate that, in the NJL model, the diquark coupling strength G_D cannot be very large, and it should be smaller than the coupling strength G_S in the quark-antiquark channel. However, it is worth to mention that the appearance of the diquark condensate in the vacuum may be a consequence of the lack of deconfinement in the NJL model.

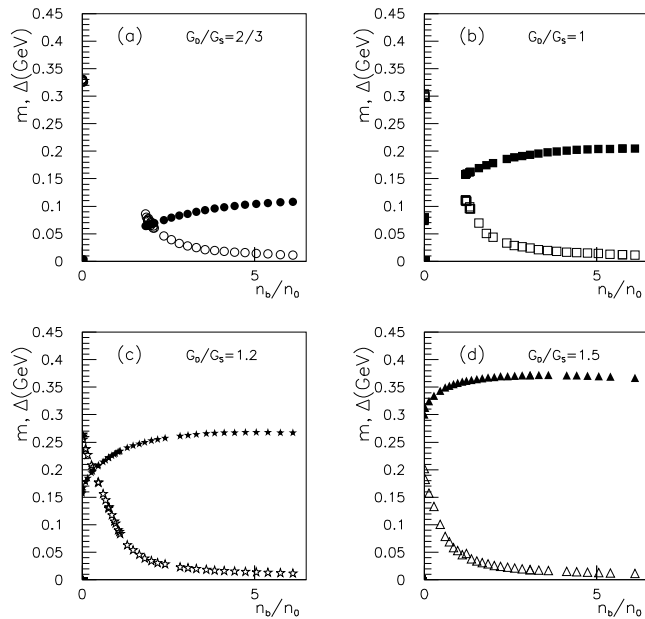


FIG. 2. The two gaps m (white points) and Δ (black points) as functions of scaled baron density n_b/n_0 for $G_D/G_S = 2/3, 1, 1.2, 1.5$, respectively. Where n_0 is the normal nuclear matter density.

We summarize the phase structure along the chemical potential direction: 1) when $\mu < \mu_\Delta$, the chiral symmetry is broken; 2) in the regime from μ_Δ to μ_χ , both chiral and color symmetries are broken, and 3) when $\mu > \mu_\chi$, the chiral symmetry restores partially and the phase is dominated by the color superconductivity. The phase structure depends on the magnitude of G_D/G_S . If G_D/G_S is very small, the diquark condensate will never appear; If $G_D/G_S < 1$ but not too small, there will be no double broken phase, the chiral phase transition and the color superconductivity phase transition occur at the same critical point $\mu_\chi = \mu_\Delta$. With increasing of G_D/G_S , the diquark condensate starts to appear at smaller μ_Δ and the chiral symmetry restores at smaller μ_χ , and the width of the double broken phase, $\mu_\chi - \mu_\Delta$, increases.

Competition between the chiral and diquark condensates

In order to understand the competition mechanism and explicitly show how the diquark condensate influences the chiral phase transition, let us analyze Fig. 1 in more detail. In the case of $G_D/G_S = 0$, only chiral phase transition occurs, the thermal system in the mean-field approximation is nearly a free Fermi gas made of constituent quarks. In the limit of $T = 0$, there is a very sharp Fermi surface of the constituent quark. When the chemical potential is larger than the constituent quark mass in the vacuum, the chiral symmetry restores, and the system of constituent quarks becomes a system of current quarks. When a diquark gap Δ forms in the case of $G_D/G_S \neq 0$, it will smooth the sharp Fermi surface of the constituent quark. In other words, the diquark pair lowers the sharp Fermi surface, and induces a smaller critical chemical potential of chiral restoration.

In TABLE I, we list the chemical potentials μ_Δ , at which the diquark gap starts appearing, and μ_χ , at which the chiral symmetry restores, for different values of G_D/G_S . $\mu_F^0 = 345.3$ MeV is the critical chemical potential in the case of $G_D/G_S = 0$. Δ_χ is the value of diquark gap at μ_χ , if there is a jump, it is the lower value.

G_D/G_S	μ_Δ (MeV)	μ_χ (MeV)	$\mu_\chi - \mu_\Delta$ (MeV)	Δ_χ (MeV)	$(\mu_F^0 - \mu_\chi)/\Delta_\chi$	$(\mu_F^0 - \mu_\Delta)/\Delta_\chi$
1	298	304.8	6	82	0.49	0.57
1.2	242	266	24	162	0.49	0.64
1.5	70	190	120	310	0.50	0.89

TABLE I. The G_D dependence of chemical potentials μ_Δ and μ_χ , $\mu_F^0 = 345.3$ MeV.

We see that for larger G_D/G_S , the diquark condensate appears at a smaller chemical potential μ_Δ , and the chiral phase transition occurs at a smaller critical chemical potential μ_χ , the gap of the diquark condensate Δ_χ at μ_χ becomes larger, and the regime of the double broken phase becomes wider.

We assume the relation between Δ_χ and μ_χ as

$$\mu_\chi = \mu_F^0 - x\Delta_\chi, \quad (2.57)$$

and the relation between Δ_χ and μ_Δ as

$$\mu_\Delta = \mu_F^0 - y\Delta_\chi. \quad (2.58)$$

In TABLE I, we listed the values of $x = (\mu_F^0 - \mu_\chi)/\Delta_\chi$ and $y = (\mu_F^0 - \mu_\Delta)/\Delta_\chi$ for different G_D/G_S . It is found that x is almost G_D/G_S independent and equal to 1/2. As for y , it is larger than 1/2 and increases with increasing of G_D/G_S . From the Eqs. (2.57) and (2.58), we have the relation

$$\mu_\chi - \mu_\Delta = (y - 1/2)\Delta_\chi \quad (2.59)$$

for the double broken phase. With increasing of G_D/G_S , y and Δ_χ increase, and then the width of the double broken phase, $\mu_\chi - \mu_\Delta$, becomes larger.

Now we turn to study how the chiral gap influences the color superconductivity phase transition. Firstly, we change the constituent quark mass in the vacuum from 330 MeV to 486 MeV. To fit the pion properties, the coupling constant in the quark-antiquark channel is correspondingly increased from G_S to $1.2G_S$. We plot the diquark gap as a function of μ in Fig. 3a for the two vacuum masses and for $G_D/G_S = 2/3, 1, 1.2, 1.5$. We find that for the same G_D/G_S , the diquark gap starts to appear at much larger chemical potential μ_Δ when the vacuum mass increases from 330 MeV to 486 MeV.

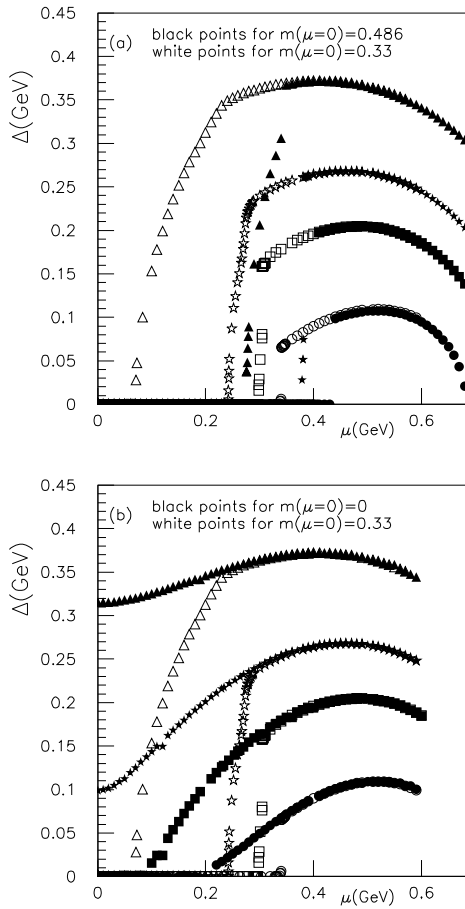


FIG. 3. The influence of chiral gap on the color superconductivity phase transition in the case of $m(\mu = 0) = 486\text{MeV}$ in (a) and $m(\mu = 0) = 0$ in (b).

Then we withdraw the quark mass, i.e., taking $m = 0$ even in the vacuum (this, of course, is artificial). We plot the diquark gap as a function of μ in Fig. 3 b for $m(\mu = 0) = 0$ and 330 MeV and for $G_D/G_S = 2/3, 1, 1.2, 1.5$. We find that for any G_D/G_S , the diquark condensate starts to appear at a much smaller chemical potential μ_Δ for $m(\mu = 0) = 0$ compared with $m(\mu = 0) = 330\text{ MeV}$.

From Fig. 3 a and b, we can see that the vacuum quark mass only changes the critical

point of color superconductivity μ_Δ , the diquark gaps for different vacuum quark masses coincide in the overlap regime of the color superconductivity phase, where chiral symmetry restores partially.

From the influence of the diquark gap on the chiral phase transition and the influence of the chiral gap on the color superconductivity phase transition, it is found that there does exist a strong competition between the two phases. The competition starts at μ_Δ and ends at μ_χ . We call the double broken phase as the competition regime, which becomes wider with increasing of G_D/G_S . This competition regime is the result of the diquark gap smoothing the sharp Fermi surface of the constituent quark. If the attractive interaction in the diquark channel is too small, there will be no diquark pairs, the system will be in the chiral breaking phase before μ_χ , and in the chiral symmetry restoration phase after μ_χ . If the attractive interaction in the diquark channel is strong enough, diquark pairs can be formed and smooth the sharp Fermi surface, and induce a smaller critical chemical potential of chiral symmetry restoration.

The influence of color breaking on quark properties

Finally, we study how the diquark condensate influences the quark properties. In the normal phase, the quarks in different colors are degenerate. However, in the color breaking phase, the red and green quarks are involved in the diquark condensate, while the blue quarks do not.

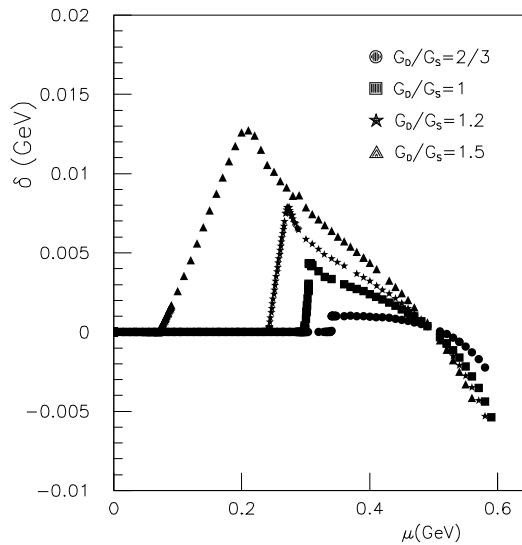


FIG. 4. The difference of the chiral condensates for quarks in different colors δ as a function of the chemical potential μ with respect to $G_D/G_S = 2/3, 1, 1.2, 1.5$, respectively.

The quark mass m appeared in the formulae of this section is the mass for the third quark which does not participate in the diquark condensate. We have seen that the diquark condensate influences much the quark mass m in the competition regime $\mu_\Delta < \mu < \mu_\chi$. In

the color breaking phase, i.e., when $\mu > \mu_\Delta$, the quark mass m in different cases of G_D decreases slowly with increasing μ , and reaches the same value at about $\mu = 500$ MeV.

The difference of the chiral condensates for quarks in different colors δ defined in Eq. (2.38) is shown in Fig. 4 as a function of the chemical potential μ with respect to $G_D/G_S = 2/3, 1, 1.2, 1.5$. It is found that in any case δ is zero before μ_Δ , then begins to increase at μ_Δ and reaches its maximum at μ_χ , and starts to decrease after $\mu > \mu_\chi$, and approaches to zero at about $\mu = 500$ MeV, when $\mu > 500$ MeV, δ becomes negative. With increasing G_D , $\delta(\mu_\chi)$ increases from 1 MeV for $G_D/G_S = 2/3$ to 13 MeV for $G_D/G_S = 1.5$. Comparing with the magnitude of the diquark condensate, δ is relatively small in the color superconductivity phase.

Summary of this section

In the mean-field approximation of the extended NJL model, considering only the attractive interactions in the 0^+ color singlet quark-antiquark channel and in the color anti-triplet diquark channel, the Nambu-Gorkov form of the quark propagator has been evaluated with a dynamical quark mass. The Nambu-Gorkov massive propagator makes it possible to extend the Green-function approach to the moderate baryon density regime. The familiar expression of the thermodynamic potential has been re-evaluated by using the massive quark propagator.

The phase structure along the chemical potential direction has been investigated. The system is in the chiral symmetry breaking phase below μ_Δ , in the color superconducting phase above μ_χ , and the two phases compete with each other in the double broken phase with width $\mu_\chi - \mu_\Delta$. The existence of the double broken phase depends on the magnitude of G_D/G_S . If $G_D < G_S$, there is no double broken phase, the chiral phase transition and the color superconductivity phase transition occur at the same chemical potential. The double broken phase starts to appear when $G_D/G_S \simeq 1$, and the regime of this phase becomes wider when the diquark coupling strength increases.

The double broken phase is a consequence of the competition between the chiral condensate and the diquark condensate. The competition mechanism has been analyzed by investigating the influence of the diquark condensate on the sharp Fermi surface of the constituent quark. The diquark condensate smoothes the sharp Fermi surface, and induces the chiral phase transition and the color superconducting phase transition occurring at smaller critical chemical potentials. The stronger the diquark coupling strength is, the smaller critical chemical potential (or the critical baryon number density) will be for the appearance of the diquark condensate.

However, it is found that when $G_D/G_S \geq 1$, the diquark condensate appears even in the vacuum. It indicates a nonzero Majorana mass for quarks in the vacuum, which would be in conflict with the standard definition of the bayron number in the vacuum. This unphysical result may suggest that in the NJL model, the diquark coupling strength G_D cannot be very large. For the parameters of the NJL model used in this section, our results suggest that the diquark coupling strength should be smaller than the coupling strength G_S in the quark-antiquark channel. Correspondingly, the upper limit of the diquark gap parameter Δ is about 200 MeV. It is also worth to mention that the appearance of the diquark condensate in the vacuum may be a result of the lack of deconfinement in the NJL model.

III. THE GAPLESS 2SC PHASE

In the previous section, we discussed the phase transition from the hadronic phase to the color superconducting phase. Now we are going to discuss the two-flavor color superconducting phase under the local charge neutrality condition based on Refs. [87–89,121].

It is very likely that the color superconducting phase may exist in the core of compact stars, where bulk matter should satisfy the charge neutrality condition. This is because bulk matter inside the neutron star is bound by the gravitation force, which is much weaker than the electromagnetic and the strong color forces. Any electric charges or color charges will forbid the formation of bulk matter. In addition, matter inside neutron star also needs to satisfy the β -equilibrium.

In the ideal two-flavor color superconducting (2SC) phase, the pairing u and d quarks have the same Fermi momenta. Because u quark carries electric charge $2/3$, and d quark carries electric charge $-1/3$, it is easy to check that quark matter in the ideal 2SC phase is positively charged. To satisfy the electric charge neutrality condition, roughly speaking, twice as many d quarks as u quarks are needed. This induces a large difference between the Fermi surfaces of the two pairing quarks, i.e., $\mu_d - \mu_u = \mu_e \approx \mu/4$, where μ, μ_e are chemical potentials for quarks and electrons, respectively. Naively, one would expect that the requirement of the charge neutrality condition will destroy the ud Cooper pairing in the 2SC phase.

Indeed, the interest in the charge neutral 2SC phase was stirred by the paper Ref. [119]. It was claimed in this paper that there will be no 2SC phase inside neutron star under the requirement of the charge neutrality condition. In fact, the authors meant that for a charge neutral three flavor system, the 2SC+s phase is not favorable compared to the CFL phase. This is a natural result under the assumption of a *small* strange quark mass, even without the requirement of the charge neutrality condition. In the framework of the bag model, in which the strange quark mass is very small, the CFL phase is always the ground state for cold dense quark matter, and there is no space for the existence of two-flavor quark matter.

However, there is another scenario about the hadron-quark phase transition in the framework of the SU(3) NJL model. In the vacuum, quarks obtain their dynamical masses induced by the chiral condensate. u, d quarks have constituent mass around 330MeV, while the s quark has heavier constituent mass, which is around 500MeV. With the increasing of the bayron density, the constituent quark mass starts to decrease when the chemical potential becomes larger than its vacuum constituent mass. In this scenario, s quark restores chiral symmetry at a larger critical chemical potential than that of u, d quarks. If the deconfinement phase transition happens sequentially, there will exist some baryon density regime for only u, d quark matter and s quark is still too heavy to appear in the system.

It is worth to mention that the effect of the electric charge neutrality condition on a three-flavor quark system is very different from that on a two-flavor quark system. Because s quark carries $-1/3$ electric charges, it is much easier to neutralize the electric charges in a three-flavor quark system than that in a two-flavor quark system. However, the color charge neutrality condition is nontrivial in a three-flavor quark system, when the strange quark mass is not very small. For a detailed consideration of the charge neutral three-flavor system, see recent papers Refs. [90–93].

In the following, we focus on the charge neutral two flavor quark system. Motivated by

the sequential deconfinement scenario, the authors of Ref. [120] investigated charge neutral quark matter based on the SU(3) NJL model. To large extent, their results agree with those in Ref. [119], i.e., the CFL phase is more favorable than the 2SC+s phase in charge neutral three-flavor cold dense quark matter, and they did not find the charge neutral 2SC phase.

However, it was found in Ref. [121] that a charge neutral two-flavor color superconducting (N2SC) phase does exist, which was confirmed in Refs. [122,123]. Comparing with the ideal 2SC phase, the N2SC phase found in Ref. [121] has a largely reduced diquark gap parameter, and the pairing quarks have different number densities. The latter contradicts the paring ansatz in Ref. [124]. Therefore, one could suggest that this phase is an unstable Sarma state [125]. In Ref. [87], it was shown that the N2SC phase is a stable state under the restriction of the charge neutrality condition. As a by-product, which comes out as a very important feature, it was found that the quasi-particle spectrum has zero-energy excitation in this charge neutral two-flavor color superconducting phase. Thus this phase was named the “gapless 2SC(g2SC)” phase.

In the following of this section, firstly, using the method introduced in the previous section, I will derive the thermodynamic potential for the charge neutral two-flavor quark system based on Ref. [121]. Then I discuss the ground state of the charge neutral two-flavor quark system and introduce the g2SC phase [87]. At last, I show the properties of the g2SC phase at zero as well as at nonzero temperatures [88], and the color screening properties [89] in the g2SC phase.

A. Thermodynamic potential of the neutral two-flavor quark system

We consider the SU(2) NJL model by assuming that the strange quark does not appear in the system, and we only consider scalar, pseudoscalar mesons and scalar diquark. The Lagrangian density has the same form as Eq. (2.1). As it was shown in Ref. [45,102], in the color superconducting phase, the small quark mass due to the explicit chiral symmetry breaking has little effect on the diquark condensate. Therefore, for simplicity, in this section, we only consider the chiral limit case $m_0 = 0$, and the parameters G_S and Λ in the chiral limit are fixed as

$$G_S = 5.0163 \text{GeV}^{-2}, \Lambda = 0.6533 \text{GeV}. \quad (3.1)$$

The corresponding effective mass $m = 0.314 \text{GeV}$, and we still choose G_D as a free parameter with the ratio $\eta = G_D/G_S$.

The partition function of the grand canonical ensemble can be evaluated by using standard method [114,115],

$$\mathcal{Z} = N' \int [d\bar{q}] [dq] \exp \left\{ \int_0^\beta d\tau \int d^3\mathbf{x} (\tilde{\mathcal{L}} + \mu \bar{q} \gamma_0 q) \right\}, \quad (3.2)$$

where $\beta = 1/T$ is the inverse of the temperature T , and μ is the chemical potential. When the electric and color charge neutrality conditions are considered, the chemical potential μ is a diagonal 6×6 matrix in flavor and color space, and can be expressed as

$$\mu = \text{diag}(\mu_{ur}, \mu_{ug}, \mu_{ub}, \mu_{dr}, \mu_{dg}, \mu_{db}), \quad (3.3)$$

the chemical potential for each color and flavor quark is specified by its electric and color charges

$$\mu_{ij,\alpha\beta} = (\mu\delta_{ij} - \mu_e Q_{ij})\delta_{\alpha\beta} + \frac{2}{\sqrt{3}}\mu_8\delta_{ij}(T_8)_{\alpha\beta}, \quad (3.4)$$

where Q and T_8 are generators of $U(1)_Q$ and $U(1)_8$. Here we assumed $\mu_3 = 0$, because the diquark condenses in the anti-blue direction, and the red and green colored quarks are degenerate. For the same flavor, the difference of chemical potentials between the red and green quarks and the blue quark is induced by μ_8 . While for the same color, the difference of chemical potentials between u and d is induced by μ_e .

The explicit expressions for each color and flavor quark chemical potential are given as:

$$\begin{aligned} \mu_{ur} &= \mu_{ug} = \mu - \frac{2}{3}\mu_e + \frac{1}{3}\mu_8, \\ \mu_{dr} &= \mu_{dg} = \mu + \frac{1}{3}\mu_e + \frac{1}{3}\mu_8, \\ \mu_{ub} &= \mu - \frac{2}{3}\mu_e - \frac{2}{3}\mu_8, \\ \mu_{db} &= \mu + \frac{1}{3}\mu_e - \frac{2}{3}\mu_8. \end{aligned} \quad (3.5)$$

For the convenience of calculations, we define the mean chemical potential $\bar{\mu}$ for the pairing quarks q_{ur}, q_{dg} , and q_{ug}, q_{dr}

$$\bar{\mu} = \frac{\mu_{ur} + \mu_{dg}}{2} = \frac{\mu_{ug} + \mu_{dr}}{2} = \mu - \frac{1}{6}\mu_e + \frac{1}{3}\mu_8, \quad (3.6)$$

and the difference of the chemical potential $\delta\mu$

$$\delta\mu = \frac{\mu_{dg} - \mu_{ur}}{2} = \frac{\mu_{dr} - \mu_{ug}}{2} = \mu_e/2. \quad (3.7)$$

Because the blue quarks do not participate in the diquark condensate, the partition function can be written as a product of three parts,

$$\mathcal{Z} = \mathcal{Z}_{const}\mathcal{Z}_b\mathcal{Z}_{rg}. \quad (3.8)$$

Where the constant part is

$$\mathcal{Z}_{const} = N' \exp\left\{-\int_0^\beta d\tau \int d^3\mathbf{x} \left[\frac{\sigma^2}{4G_S} + \frac{\Delta^* \Delta}{4G_D}\right]\right\}, \quad (3.9)$$

\mathcal{Z}_b part is for the unpairing blue quarks, and \mathcal{Z}_{rg} part is for the quarks participating in pairing. In the following, we will derive the contributions of \mathcal{Z}_b and \mathcal{Z}_{rg} .

Calculation of \mathcal{Z}_b

Introducing the 8-spinors for q_{ub} and q_{db} ,

$$\bar{\Psi}_b = (\bar{q}_{ub}, \bar{q}_{db}; \bar{q}_{ub}^C, \bar{q}_{db}^C), \quad (3.10)$$

we can express \mathcal{Z}_b as

$$\begin{aligned}\mathcal{Z}_b &= \int [d\Psi_b] \exp\left\{\frac{1}{2} \sum_{n,\mathbf{p}} \bar{\Psi}_b \frac{[G_0^{-1}]_b}{T} \Psi_b\right\} \\ &= \text{Det}^{1/2}(\beta[G_0^{-1}]_b),\end{aligned}\quad (3.11)$$

where the determinantal operation Det is to be carried out over the Dirac, color, flavor and the momentum-frequency space, and $[G_0^{-1}]_b$ has the form of

$$[G_0^{-1}]_b = \begin{pmatrix} [G_0^+]_{ub}^{-1} & 0 & 0 & 0 \\ 0 & [G_0^+]_{db}^{-1} & 0 & 0 \\ 0 & 0 & [G_0^-]_{ub}^{-1} & 0 \\ 0 & 0 & 0 & [G_0^-]_{db}^{-1} \end{pmatrix}, \quad (3.12)$$

with

$$[G_0^\pm]_{i\alpha}^{-1} = \not{p} \pm \not{\mu}_{i\alpha} - m. \quad (3.13)$$

Here we have used $\not{p} = p_\mu \gamma^\mu$ and $\not{\mu}_{i\alpha} = \mu_{i\alpha} \gamma_0$.

For the two blue quarks not participating in the diquark condensate, from Eq. (3.11), one can have

$$\begin{aligned}\ln \mathcal{Z}_b &= \frac{1}{2} \ln \text{Det}(\beta[G_0^{-1}]_b) \\ &= \frac{1}{2} \ln [\text{Det}(\beta[G_0^+]_{ub}^{-1}) \text{Det}(\beta[G_0^-]_{ub}^{-1})] [\text{Det}(\beta[G_0^+]_{db}^{-1}) \text{Det}(\beta[G_0^-]_{db}^{-1})].\end{aligned}\quad (3.14)$$

Using the results of Eq. (2.42) in the previous section, one has

$$\begin{aligned}[\text{Det}(\beta[G_0^+]_{ub}^{-1}) \text{Det}(\beta[G_0^-]_{ub}^{-1})] &= \beta^4 [p_0^2 - E_{ub}^{+2}] [p_0^2 - E_{ub}^{-2}], \\ [\text{Det}(\beta[G_0^+]_{db}^{-1}) \text{Det}(\beta[G_0^-]_{db}^{-1})] &= \beta^4 [p_0^2 - E_{db}^{+2}] [p_0^2 - E_{db}^{-2}],\end{aligned}\quad (3.15)$$

with $E_{ub}^\pm = E \pm \mu_{ub}$ and $E_{db}^\pm = E \pm \mu_{db}$ where $E = \sqrt{\mathbf{p}^2 + m^2}$. Considering the determinant in the flavor, color, spin spaces and the momentum-frequency space, we get the expression

$$\begin{aligned}\ln \mathcal{Z}_b &= \sum_n \sum_{\mathbf{p}} \{ \ln(\beta^2 [p_0^2 - (E_{ub}^+)^2]) + \ln(\beta^2 [p_0^2 - (E_{ub}^-)^2]) \\ &\quad + \ln(\beta^2 [p_0^2 - (E_{db}^+)^2]) + \ln(\beta^2 [p_0^2 - (E_{db}^-)^2]) \}.\end{aligned}\quad (3.16)$$

Calculation of \mathcal{Z}_{rg}

The calculation of \mathcal{Z}_{rg} here is much more complicated than that when the two pairing quarks have the same Fermi momonta [51]. Also, we introduce the Nambu-Gokov formalism for q_{ur}, q_{ug}, q_{dr} and q_{dg} , i.e.,

$$\bar{\Psi} = (\bar{q}_{ur}, \bar{q}_{ug}, \bar{q}_{dr}, \bar{q}_{dg}; \bar{q}_{ur}^C, \bar{q}_{ug}^C, \bar{q}_{dr}^C, \bar{q}_{dg}^C). \quad (3.17)$$

The \mathcal{Z}_{rg} can have the simple form as

$$\begin{aligned}\mathcal{Z}_{rg} &= \int [d\Psi] \exp\left\{\frac{1}{2} \sum_{n,\mathbf{p}} \bar{\Psi} \frac{G_{rg}^{-1}}{T} \Psi\right\} \\ &= \text{Det}^{1/2}(\beta G_{rg}^{-1}),\end{aligned}\quad (3.18)$$

where

$$G_{rg}^{-1} = \begin{pmatrix} [G_0^+]_{rg}^{-1} & \Delta^- \\ \Delta^+ & [G_0^-]_{rg}^{-1} \end{pmatrix}, \quad (3.19)$$

with

$$[G_0^\pm]_{rg}^{-1} = \begin{pmatrix} [G_0^\pm]_{ur}^{-1} & 0 & 0 & 0 \\ 0 & [G_0^\pm]_{ug}^{-1} & 0 & 0 \\ 0 & 0 & [G_0^\pm]_{dr}^{-1} & 0 \\ 0 & 0 & 0 & [G_0^\pm]_{dg}^{-1} \end{pmatrix}, \quad (3.20)$$

and the matrix form for Δ^\pm is

$$\Delta^- = -i\Delta\gamma_5 \begin{pmatrix} 0 & 0 & 0 & 1 \\ 0 & 0 & -1 & 0 \\ 0 & -1 & 0 & 0 \\ 1 & 0 & 0 & 0 \end{pmatrix}, \quad \Delta^+ = \gamma^0(\Delta^-)^\dagger\gamma^0. \quad (3.21)$$

From Eq. (3.18), one obtains

$$\ln \mathcal{Z}_{rg} = \frac{1}{2} \ln \text{Det}(\beta G_{rg}^{-1}). \quad (3.22)$$

Using the identity Eq. (2.45), one can have

$$\begin{aligned}\text{Det}(G_{rg}^{-1}) &= \text{Det}D_1 = \text{Det}(-\Delta^+\Delta^- + \Delta^+[G_0^+]_{rg}^{-1}[\Delta^-]^{-1}[G_0^-]_{rg}^{-1}) \\ &= \text{Det}D_2 = \text{Det}(-\Delta^-\Delta^+ + \Delta^-[G_0^-]_{rg}^{-1}[\Delta^+]^{-1}[G_0^+]_{rg}^{-1}).\end{aligned}\quad (3.23)$$

Using the massive energy projectors Λ_\pm in Eq. (2.21) for each flavor and color quark, we can work out the diagonal matrix D_1 and D_2 as

$$\begin{aligned}(D_1)_{11} &= (D_1)_{22} = [(p_0 + \delta\mu)^2 - [E_\Delta^-]^2]\Lambda_- + [(p_0 + \delta\mu)^2 - [E_\Delta^+]^2]\Lambda_+ \\ (D_1)_{33} &= (D_1)_{44} = [(p_0 - \delta\mu)^2 - [E_\Delta^-]^2]\Lambda_- + [(p_0 - \delta\mu)^2 - [E_\Delta^+]^2]\Lambda_+ \\ (D_2)_{11} &= (D_2)_{22} = [(p_0 - \delta\mu)^2 - [E_\Delta^+]^2]\Lambda_- + [(p_0 - \delta\mu)^2 - [E_\Delta^-]^2]\Lambda_+ \\ (D_2)_{33} &= (D_2)_{44} = [(p_0 + \delta\mu)^2 - [E_\Delta^+]^2]\Lambda_- + [(p_0 + \delta\mu)^2 - [E_\Delta^-]^2]\Lambda_+, \end{aligned}\quad (3.24)$$

where $E_\Delta^\pm = \sqrt{(E \pm \bar{\mu})^2 + \Delta^2}$.

With the above equations, Eq. (3.22) can be expressed as

$$\begin{aligned}\ln \mathcal{Z}_{rg} &= 2 \sum_n \sum_p \{ \ln[\beta^2(p_0^2 - (E_\Delta^- + \delta\mu))^2] + \ln[\beta^2(p_0^2 - (E_\Delta^- - \delta\mu))^2] \\ &\quad + \ln[\beta^2(p_0^2 - (E_\Delta^+ + \delta\mu))^2] + \ln[\beta^2(p_0^2 - (E_\Delta^+ - \delta\mu))^2] \}.\end{aligned}\quad (3.25)$$

The thermodynamic potential

Using the helpful relation Eq. (2.50), one can evaluate the thermodynamic potential of the quark system in the mean-field approximation. The total thermodynamic potential for u, d quarks in β -equilibrium with electrons takes the form [121,87,88]:

$$\begin{aligned}\Omega_{u,d,e} = & -\frac{1}{12\pi^2} \left(\mu_e^4 + 2\pi^2 T^2 \mu_e^2 + \frac{7\pi^4}{15} T^4 \right) + \frac{m^2}{4G_S} \\ & + \frac{\Delta^2}{4G_D} - \sum_a \int \frac{d^3 p}{(2\pi)^3} [E_a + 2T \ln (1 + e^{-E_a/T})],\end{aligned}\quad (3.26)$$

where the electron mass was taken to be zero, which is sufficient for the purposes of the current study. The sum in the second line of Eq. (3.26) runs over all (6 quark and 6 antiquark) quasi-particles. The explicit dispersion relations and the degeneracy factors of the quasi-particles read

$$E_{ub}^\pm = E(p) \pm \mu_{ub}, \quad [\times 1] \quad (3.27)$$

$$E_{db}^\pm = E(p) \pm \mu_{db}, \quad [\times 1] \quad (3.28)$$

$$E_{\Delta^\pm}^\pm = E_\Delta^\pm(p) \pm \delta\mu. \quad [\times 2] \quad (3.29)$$

B. Gap equations and number densities

From the thermodynamic potential Eq. (3.26), we can derive the gap equations of the order parameters m and Δ for the chiral and color superconducting phase transitions, as well as the number densities for quarks with different color and flavor.

Gap equation for the quark mass

The gap equation for the quark mass can be derived by using

$$\frac{\partial \Omega_{u,d,e}}{\partial m} = 0. \quad (3.30)$$

The explicit expression for the above equation is

$$\begin{aligned}m = & 4G_S \int \frac{d^3 \mathbf{p}}{(2\pi)^3} \frac{m}{E} \left[2 \frac{E - \bar{\mu}}{E_\Delta^-} [1 - \tilde{f}(E_{\Delta^+}) - \tilde{f}(E_{\Delta^-})] \right. \\ & + 2 \frac{E + \bar{\mu}}{E_\Delta^+} [1 - \tilde{f}(E_{\Delta^+}^+) - \tilde{f}(E_{\Delta^-}^+)] \\ & \left. + 2 - \tilde{f}(E_{ub}^+) - \tilde{f}(E_{ub}^-) - \tilde{f}(E_{db}^+) - \tilde{f}(E_{db}^-) \right].\end{aligned}\quad (3.31)$$

In the chiral limit, the trivial solution $m = 0$ corresponds to a chirally symmetric phase of quark matter, while a nontrivial solution $m \neq 0$ corresponds to a phase with spontaneously broken chiral symmetry.

Gap equation for the diquark gap

Similarly, the gap equation for the diquark condensate can be derived using

$$\frac{\partial \Omega_{u,d,e}}{\partial \Delta} = 0, \quad (3.32)$$

the explicit expression has the form

$$\begin{aligned} \Delta [1 - 4G_D \int \frac{d^3 \mathbf{p}}{(2\pi)^3} [2 \frac{1}{E_\Delta^-} (1 - \tilde{f}(E_{\Delta^+}^-) - \tilde{f}(E_{\Delta^-}^-)) \\ + 2 \frac{1}{E_\Delta^+} (1 - \tilde{f}(E_{\Delta^+}^+) - \tilde{f}(E_{\Delta^-}^+))] = 0. \end{aligned} \quad (3.33)$$

This equation can also have trivial as well as nontrivial solutions for Δ , and the nontrivial solution $\Delta \neq 0$ corresponds to a color superconducting phase.

Number densities of quarks

According to one of the criteria of the g2SC phase, the densities of the quark species that participate in pairing dynamics are not equal at zero temperature [87,121]. This is in contrast to regular pairing in the conventional gapped color superconductors [124].

The quark densities are obtained by taking the partial derivatives of the potential $\Omega_{u,d,e}$ in Eq. (3.26) with respect to the chemical potentials for each flavor and color. Because of the residual $SU(2)_c$ symmetry in the ground state of quark matter, the densities of red and green quarks for the same flavor, are equal in the g2SC ground state. For example, the densities of the up quarks participating in the Cooper pairing read

$$\begin{aligned} n_{ur} = n_{ug} = \int \frac{d^3 \mathbf{p}}{(2\pi)^3} \left[\frac{E + \bar{\mu}}{E_\Delta^+} [1 - \tilde{f}(E_{\Delta^+}^+) - \tilde{f}(E_{\Delta^-}^+)] \right. \\ \left. - \frac{E - \bar{\mu}}{E_\Delta^-} [1 - \tilde{f}(E_{\Delta^+}^-) - \tilde{f}(E_{\Delta^-}^-)] \right. \\ \left. + \tilde{f}(E_{\Delta^+}^-) + \tilde{f}(E_{\Delta^+}^+) - \tilde{f}(E_{\Delta^-}^+) - \tilde{f}(E_{\Delta^-}^-) \right]. \end{aligned} \quad (3.34)$$

Similarly, for the densities of the down quarks, we get

$$\begin{aligned} n_{dg} = n_{dr} = \int \frac{d^3 \mathbf{p}}{(2\pi)^3} \left[\frac{E + \bar{\mu}}{E_\Delta^+} [1 - \tilde{f}(E_{\Delta^+}^+) - \tilde{f}(E_{\Delta^-}^+)] \right. \\ \left. - \frac{E - \bar{\mu}}{E_\Delta^-} [1 - \tilde{f}(E_{\Delta^+}^-) - \tilde{f}(E_{\Delta^-}^-)] \right. \\ \left. - \tilde{f}(E_{\Delta^+}^-) - \tilde{f}(E_{\Delta^+}^+) + \tilde{f}(E_{\Delta^-}^+) + \tilde{f}(E_{\Delta^-}^-) \right]. \end{aligned} \quad (3.35)$$

As we see, the densities of the up and down quarks participating in the Cooper pairing are not equal. In fact, the difference of the densities is given by

$$\begin{aligned} n_{dg} - n_{ur} = n_{dr} - n_{ug} \\ = 2 \int \frac{d^3 \mathbf{p}}{(2\pi)^3} \left[\tilde{f}(E_{\Delta^-}^-) - \tilde{f}(E_{\Delta^+}^-) + \tilde{f}(E_{\Delta^-}^+) - \tilde{f}(E_{\Delta^+}^+) \right], \end{aligned} \quad (3.36)$$

which is always nonzero at finite temperature provided the mismatch parameter $\delta\mu$ is nonzero. It is even more important for us here that this difference is nonzero at zero temperature in the g2SC phase of quark matter,

$$\begin{aligned} (n_{dg} - n_{ur})|_{T=0} &= (n_{dr} - n_{ug})|_{T=0} \\ &= \theta(\delta\mu - \Delta) \frac{2}{3\pi^2} \sqrt{(\delta\mu)^2 - \Delta^2} (3\bar{\mu}^2 + (\delta\mu)^2 - \Delta^2). \end{aligned} \quad (3.37)$$

This is in contrast to the 2SC phase ($\delta\mu < \Delta$) where this difference is zero in agreement with the arguments of Ref. [124].

The unpaired blue quarks, u_b and d_b , are singlet states with respect to $SU(2)_c$ symmetry of the ground state. The densities of these quarks are

$$n_{ub} = 2 \int \frac{d^3\mathbf{p}}{(2\pi)^3} [\tilde{f}(E_{ub}^-) - \tilde{f}(E_{ub}^+)] \simeq \frac{\mu_{ub}}{3} \left(\frac{\mu_{ub}^2}{\pi^2} + T^2 \right), \quad (3.38)$$

for the up quarks, and

$$n_{db} = 2 \int \frac{d^3\mathbf{p}}{(2\pi)^3} [\tilde{f}(E_{db}^-) - \tilde{f}(E_{db}^+)] \simeq \frac{\mu_{db}}{3} \left(\frac{\mu_{db}^2}{\pi^2} + T^2 \right), \quad (3.39)$$

for the down quarks, respectively.

C. The charge neutral ground state and the g2SC phase

If a macroscopic chunk of quark matter exists inside compact stars, it must be neutral with respect to electric as well as color charges.

electric and color charge neutrality

It has been shown that, in QCD case, the two-flavor color superconductivity is automatically color neutral, because of a non-vanishing expectation value of the 8th gluon field, for more details, see Refs. [126,127]. However, in the framework of the NJL model which lacks gluons, the color charge neutrality condition is to choose μ_8 such that the system has zero net charge n_8 , i.e.,

$$\begin{aligned} n_8 = \frac{4}{3} \int \frac{d^3\mathbf{p}}{(2\pi)^3} &\left[-\frac{E - \bar{\mu}}{E_\Delta^-} [1 - \tilde{f}(E_{\Delta^+}^-) - \tilde{f}(E_{\Delta^-}^-)] \right. \\ &+ \frac{E + \bar{\mu}}{E_\Delta^+} [1 - \tilde{f}(E_{\Delta^+}^+) - \tilde{f}(E_{\Delta^-}^+)] \\ &\left. + \tilde{f}(E_{ub}^+) - \tilde{f}(E_{ub}^-) + \tilde{f}(E_{db}^+) - \tilde{f}(E_{db}^-) \right]. \end{aligned} \quad (3.40)$$

The detailed numerical calculation in Ref. [121] shows that it is very easy to satisfy the color neutrality condition, μ_8 is around several MeV, which is very small comparing with the quark chemical potential μ . In the following discussions, color charge neutrality condition is always satisfied.

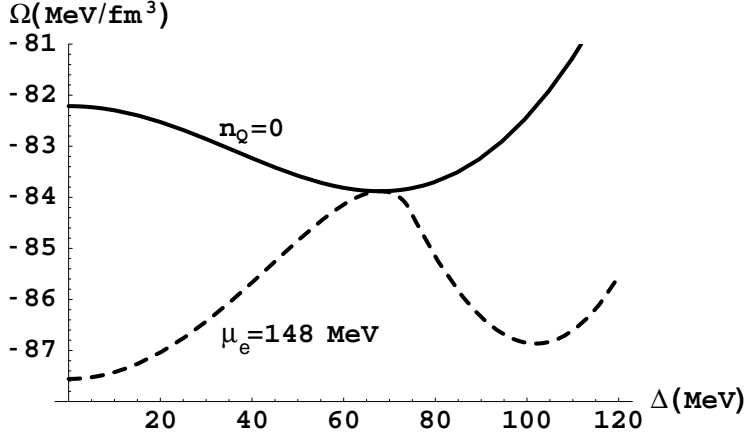


FIG. 5. The effective potential as a function of the diquark gap Δ calculated at a fixed value of the electric chemical potential $\mu_e = 148$ MeV (dashed line), and the effective potential defined along the neutrality line (solid line). The results are plotted for $\mu = 400$ MeV with $\eta = 0.75$.

In the two-flavor quark system, the electric neutrality plays an essential role. Similar to the color charge, the electric charge neutrality condition is to choose μ_e such that the system has zero net electric charge n_Q , i.e.,

$$n_Q = -\frac{1}{2}n_8 + \frac{\mu_e^3}{3\pi^2} + \frac{1}{3}\mu_e T^2 + 2 \int \frac{d^3\mathbf{p}}{(2\pi)^3} \left[\tilde{f}(E_{ub}^+) - \tilde{f}(E_{ub}^-) - \tilde{f}(E_{\Delta+}^-) - \tilde{f}(E_{\Delta+}^+) + \tilde{f}(E_{\Delta-}^+) + \tilde{f}(E_{\Delta-}^-) \right]. \quad (3.41)$$

To neutralize the electric charge in the homogeneous dense u, d quark matter, roughly speaking, twice as many d quarks as u quarks are needed, i.e., $n_d \simeq 2n_u$, where $n_{u,d}$ are the number densities for u and d quarks. This induces a mismatch between the Fermi surfaces of pairing quarks, i.e., $\mu_d - \mu_u = \mu_e = 2\delta\mu$, where μ_e is the electron chemical potential.

The proper way to find the charge neutral ground state

Now, we discuss the role of the electric charge neutrality condition. If a macroscopic chunk of quark matter has nonzero net electric charge density n_Q , the total thermodynamic potential for the system should be given by

$$\Omega = \Omega_{Coulomb} + \Omega_{u,d,e}, \quad (3.42)$$

where $\Omega_{Coulomb} \sim n_Q^2 V^{2/3}$ (V is the volume of the system) is induced by the repulsive Coulomb interaction. The energy density grows with increasing the volume of the system, as a result, it is almost impossible for matter inside stars to remain charged over macroscopic distances. So bulk quark matter must satisfy electric neutrality condition with $\Omega_{Coulomb}|_{n_Q=0} = 0$, and $\Omega_{u,d,e}|_{n_Q=0}$ is on the neutrality line. Under the charge neutrality condition, the total thermodynamic potential of the system is $\Omega|_{n_Q=0} = \Omega_{u,d,e}|_{n_Q=0}$.

Here, we want to emphasize that: *The proper way to find the ground state of homogeneous neutral u, d quark matter is to minimize the thermodynamic potential along the neutrality*

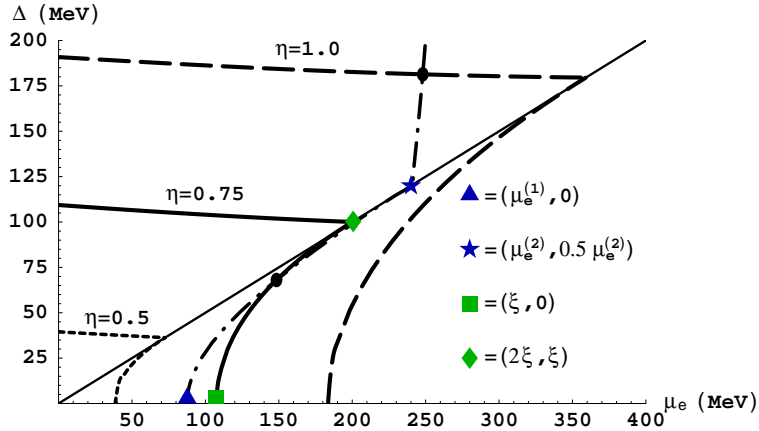


FIG. 6. The graphical representation of the solution to the charge neutrality conditions (thick dash-dotted line) and the solution to the gap equation for three different values of the diquark coupling constant (thick solid and dashed lines). The intersection points represent the solutions to both. The thin solid line divides two qualitatively different regimes, $\Delta < \delta\mu$ and $\Delta > \delta\mu$. The results are plotted for $\mu = 400$ MeV and three values of diquark coupling constant $G_D = \eta G_S$ with $\eta = 0.5$, $\eta = 0.75$, and $\eta = 1.0$.

line $\Omega|_{n_Q=0} = \Omega_{u,d,e}|_{n_Q=0}$. This is different from that in the flavor asymmetric quark system, where β -equilibrium is required but μ_e is a free parameter, and the ground state for flavor asymmetric quark matter is determined by minimizing the thermodynamic potential $\Omega_{u,d,e}$.

From Fig. 5, we can see the difference in determining the ground state for a charge neutral system and for a flavor asymmetric system when μ_e is a free parameter. In Fig. 5, at a given chemical potential $\mu = 400$ MeV and $\eta = G_D/G_S = 0.75$, the thermodynamic potential along the charge neutrality line $\Omega|_{n_Q=0}$ as a function of the diquark gap Δ is shown by the solid line. The minimum gives the ground state of the neutral system, and the corresponding values of the chemical potential and the diquark gap are $\mu_e = 148$ MeV and $\Delta = 68$ MeV, respectively. If we switch off the charge neutrality conditions, and consider the flavor asymmetric u, d quark matter in β -equilibrium like in Refs. [128,129], the electric chemical potential μ_e becomes a free parameter. At a fixed $\mu_e = 148$ MeV and with color charge neutrality, the thermodynamic potential is shown as a function of the diquark gap by the dashed line in Fig. 5. The minimum gives the ground state of the flavor asymmetric system, and the corresponding diquark gap is $\Delta = 0$, but this state has negative electric charge density, and cannot exist in the interior of compact stars.

G_D dependent charge neutral ground state and the g2SC phase

Equivalently, the neutral ground state can also be determined by solving the diquark gap equation Eq. (3.33) together with the charge neutrality conditions Eqs. (3.40) and (3.41), here we regarded the quark mass is zero in the chiral symmetric phase.

We visualize this method in Fig. 6, with color neutrality always satisfied, at a given chemical potential $\mu = 400$ MeV. The nontrivial solutions to the diquark gap equation as functions of the electric chemical potential μ_e are shown by a thick-solid line ($\eta = G_D/G_S =$

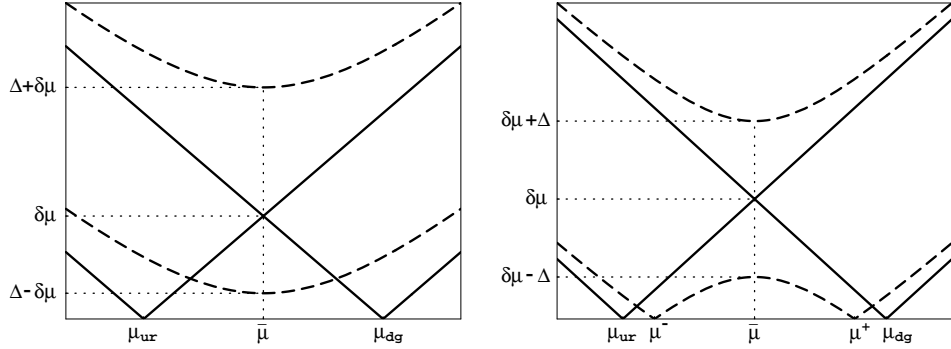


FIG. 7. The quasi-particle dispersion relations at low energies in the 2SC phase (left panel) and in the g2SC phase (right panel).

0.75), a long-dashed line ($\eta = 1.0$), and a short-dashed line ($\eta = 0.5$). It is found that for each η , the solution is divided into two branches by the thin-solid line $\Delta = \delta\mu$, and the solution is very sensitive to η . Also, there is always a trivial solution to the diquark gap equation, i.e., $\Delta = 0$. The solution of the charge neutrality conditions is shown by a thick dash-dotted line, which is also divided into two branches by the thin-solid line $\Delta = \delta\mu$, but the solution of the charge neutrality is independent of η .

The cross-point of the solutions to the charge neutrality conditions and the diquark gap gives the solution of the system. We find that the neutral ground state is sensitive to the coupling constant $G_D = \eta G_S$ in the diquark channel. In the case of a very strong coupling (e.g., $\eta = 1.0$ case), the charge neutrality line crosses the upper branch of the solution to the diquark gap, the ground state is a charge neutral regular 2SC phase with $\Delta > \delta\mu$. In the case of weak coupling (e.g., $\eta = 0.5$), the charge neutrality line crosses only the trivial solution of the diquark gap, i.e., the ground state is a charge neutral normal quark matter with $\Delta = 0$.

The regime of intermediate coupling (see, e.g., $\eta = 0.75$ case) is most interesting, the charge neutrality line crosses the lower branch of the solution of the diquark gap. It should be noticed that $\eta = 0.75$ is from the Fierz transformation, and $\eta = 2.26/3 \simeq 0.75$ obtained in the SU(2) NJL model in Ref. [106] from fitting the vacuum baryon mass. We will see that in the regime of intermediate coupling, the phase with $\Delta < \delta\mu$ is a gapless 2SC (g2SC) phase.

Quasi-particle spectrum

As we already mentioned that the pairing quarks have different number densities in the g2SC phase, which is different from the regular 2SC phase. It is the quasi-particle spectrum that makes the g2SC phase different from the gapped 2SC phase.

It is instructive to start with the excitation spectrum in the case of the ideal 2SC phase when $\delta\mu = 0$. With the conventional choice of the gap pointing in the anti-blue direction in the color space, the blue quarks are not affected by the pairing dynamics, and the other four quasi-particle excitations are linear superpositions of $u_{r,g}$ and $d_{r,g}$ quarks and holes. The quasi-particle is nearly identical with a quark at large momenta and with a hole at small momenta. We represent the quasi-particle in the form of $Q(\text{quark, hole})$, then the four quasi-particles can be represented explicitly as $Q(u_r, d_g)$, $Q(u_g, d_r)$, $Q(d_r, u_g)$ and $Q(d_g, u_r)$.

When $\delta\mu = 0$, the four quasi-particles are degenerate, and have a common gap Δ . If there is a small mismatch ($\delta\mu < \Delta$) between the Fermi surfaces of the pairing u and d quarks, the excitation spectrum will change. For example, we show the excitation spectrum of $Q(u_r, d_g)$ and $Q(d_g, u_r)$ in the left panel of Fig. 7. We can see that $\delta\mu$ induces two different dispersion relations, the quasi-particle $Q(d_g, u_r)$ has a smaller energy gap $\Delta - \delta\mu$, and the quasi-particle $Q(u_r, d_g)$ has a larger energy gap $\Delta + \delta\mu$. This is similar to the case when the mismatch is induced by the mass difference of the pairing quarks [130].

If the mismatch $\delta\mu$ is larger than the gap parameter Δ , the lower dispersion relation for the quasi-particle $Q(d_g, u_r)$ will cross the zero-energy axis, as shown in the right panel of Fig. 7. The energy of the quasi-particle $Q(d_g, u_r)$ vanishes at two values of momenta $p = \mu^-$ and $p = \mu^+$ where $\mu^\pm \equiv \bar{\mu} \pm \sqrt{(\delta\mu)^2 - \Delta^2}$. Thus this phase is called the gapless 2SC (g2SC) phase.

An unstable gapless CFL phase has been found in Ref. [130], and a similar stable gapless color superconductivity could also appear in a cold atomic gas [131] or in u, s or d, s quark matter when the number densities are kept fixed [132]. Also, some gapless phases may appear due to P-wave interactions in the cold atomic system [133].

As we shall see, the interplay of the neutrality condition and the solution to the gap equation produces some unusual properties of the g2SC phase that have no analogue in well known systems.

D. The g2SC phase at nonzero temperatures

In a superconducting system, when one increases the temperature at a given chemical potential, thermal motion will eventually break up the quark Cooper pairs. In the weakly interacting Bardeen-Copper-Schrieffer (BCS) theory, the transition between the superconducting and normal phases is usually of second order. The ratio of the critical temperature T_c^{BCS} to the zero temperature value of the gap Δ_0^{BCS} is a universal value [134]

$$r_{\text{BCS}} = \frac{T_c^{\text{BCS}}}{\Delta_0^{\text{BCS}}} = \frac{e^{\gamma_E}}{\pi} \approx 0.567, \quad (3.43)$$

where $\gamma_E \approx 0.577$ is the Euler constant. In the conventional 2SC phase of quark matter with equal densities of the up and down quarks, the ratio of the critical temperature to the zero temperature value of the gap is also the same as in the BCS theory [39]. In the spin-0 color flavor locked phase as well as in the spin-1 color spin locked phase, on the other hand, this ratio is larger than BCS ratio by the factors $2^{1/3}$ and $2^{2/3}$, respectively. These deviations are related directly to the presence of two different types of quasiparticles with nonequal gaps [65].

This commonly accepted picture of the finite temperature effects in superconducting phases changes drastically in the case of dense quark matter when the β -equilibrium and the local neutrality conditions are enforced. Below, we study this in detail.

Gap equation and charge neutrality condition

Here we consider the gap equation and charge neutrality conditions in the g2SC phase at finite temperature. Because of additional technical complications appearing at finite

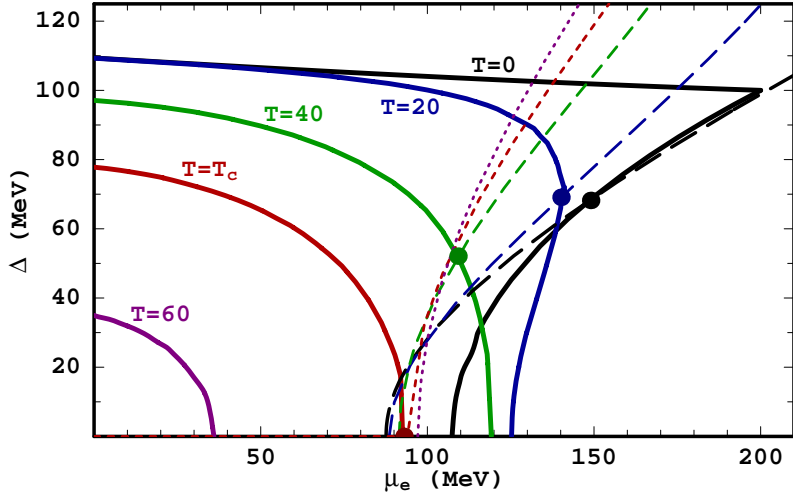


FIG. 8. The solutions to the gap equation (solid lines) and the neutrality condition (dashed lines) calculated for several values of temperature. The results are plotted for $\mu = 400$ MeV and the diquark coupling constant $G_D = \eta G_S$ with $\eta = 0.75$. In this case, $T_c \approx 50.2$ MeV.

temperature, most of the results that follow will be obtained by numerical computation. It is important to keep in mind, however, that our approach remains conceptually the same as that at zero temperature.

Before studying the gap equation (3.33), we recall that the right hand side of this equation is a function of the three chemical potentials μ , μ_e and μ_8 . The values of μ_e and μ_8 are not the free parameters in neutral quark matter. They are determined by satisfying the two charge neutrality conditions. In our analysis, on the other hand, it is very convenient to enforce only the color charge neutrality by choosing the function $\mu_8(\mu, \mu_e, \Delta)$ properly. As for the electric chemical potential μ_e , it is treated as an independent parameter at intermediate stages of calculation. Only at the very end its value is adjusted to make the quark matter also electricly neutral.

As in the case of zero temperature, the resulting color chemical potential μ_8 is much smaller than the other two chemical potentials in neutral quark matter. This, of course, is not surprising. Small nonzero values of μ_8 [typically, $\mu_8 \sim \Delta^2/\mu$] are required only because an induced color charge of the diquark condensate should be compensated. Therefore, the smallness of μ_8 is protected by the smallness of the order parameter. The numerical calculations show, in fact, that even the approximation $\mu_8 = 0$ does not modify considerably the exact solutions to the gap equation and to the electric charge neutrality condition. In practice, we either tabulate the function $\mu_8(\mu, \mu_e, \Delta)$ for a given set of parameters, or determine it numerically in the vicinity of the ground state solution.

The solutions to the gap equation (3.33) for several different values of temperature ($T = 0, 20, 40, 50.2$ and 60 MeV) are shown graphically in Fig. 8 (solid lines). The values of the temperature are marked along the curves. The results are plotted in the (μ_e, Δ) -plane. In computation we kept the quark chemical potential fixed, $\mu = 400$ MeV, and used the diquark coupling constant $G_D = \eta G_S$ with $\eta = 0.75$. This is the same choice that we used at zero temperature in Fig. 6.

Now let us briefly discuss the temperature dependence of the solution. It is not very

surprising that the shape of the graphical solution is smoothed with increasing the temperature. The same applies to the disappearance of the double-branch structure of the solution at a finite value of the temperature, $T_s \simeq 30$ MeV. Indeed, in a model that treats the electric chemical potential as a free parameter, this value of the temperature T_s marks the expected switch of two regimes. Namely, while the phase transition controlled by the μ_e parameter (i.e., neutrality is not required) is a first order phase transition at $T < T_s$, it becomes a second order phase transition at $T > T_s$.

We also observe that the value of the electric chemical potential at the point where the solution to the gap equation intersects with the μ_e -axis has a nonmonotonic dependence on the temperature. With increasing temperature, this value increases first and, after reaching some maximum value, starts to decrease and goes down to zero eventually. When the interplay with the neutrality condition is taken into account later, this simple property of the solution would produce rather unusual physical results.

We note that the temperature dependence of the solutions to the gap equation is very similar to the dependence found by Sarma in a solid state physics analogue of the g2SC phase [125]. Of course, there was no analogue of the neutrality condition in the system studied in Ref. [125]. Therefore, the mentioned similarity does not extend to the complete analysis of the g2SC phase that follows.

In Fig. 8, we also show the neutrality lines (dashed lines) for the same values of temperature ($T = 0, 20, 40, 50.2$ and 60 MeV). The convention is that the lengths of the dashes decreases with increasing the value of the temperature. As we see, with increasing temperature, the neutrality line gets steeper while its intersection point with the μ_e -axis moves towards larger values of μ_e . The points of intersection of these neutrality lines with the lines of solutions to the gap equation, when they exist, are shown as well.

As in the case of zero temperature, see Fig. 5, we need to show that the points of intersections of the gap solutions with the corresponding neutrality lines in Fig. 8 represent the ground state of the neutral quark matter. To this end, we calculate the dependence of the thermodynamic potential on the value of the gap Δ . Since the charge neutrality condition is satisfied only along the neutrality line, we restrict the thermodynamic potential only to this line. The numerical results for several values of the temperature are shown in Fig. 9.

The results at $\mu = 400$ MeV and $\eta = 0.75$ show that, for any $T < T_c \approx 50.2$ MeV, the thermodynamic potential has the global minimum away from the origin, meaning that the corresponding ground state develops a nonzero expectation value of $\Delta(T)$. Needless to say that this is the same value that one extracts from the geometrical construction in Fig. 8. The expectation value $\Delta(T)$ disappears gradually when the temperature approaches T_c from below. This is an indication of the second order phase transition. At temperature higher than T_c , the ground state of neutral quark matter is the normal phase with $\Delta(T) = 0$.

Temperature dependence of the gap

The temperature dependence of the gap is obtained by numerical solution of the gap equation (3.33) together with the two charge neutrality conditions. Of course, this is equivalent to the geometrical construction used in Fig. 8, where the intersection points of two types of lines determine the values of the gaps in the ground state.

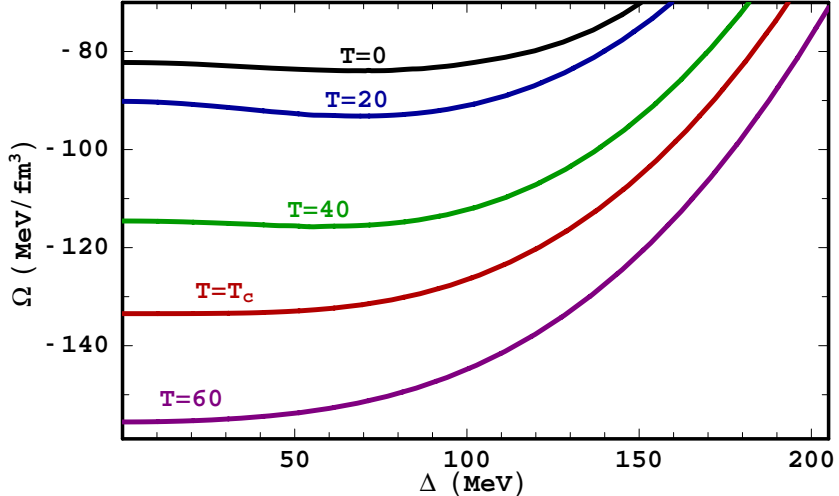


FIG. 9. The thermodynamic potential of neutral quark matter as a function of the diquark gap Δ calculated for several values of temperature.

The typical results for the default choice of parameters $\mu = 400$ MeV and $\eta = 0.75$ are shown in Fig. 10. Both the values of the diquark gap (solid line) and the mismatch parameter $\delta\mu = \mu_e/2$ (dashed line) are plotted. One very unusual property of the shown temperature dependence of the gap is the nonmonotonic behavior. Only at sufficiently high temperatures, the gap is a decreasing function. In the low temperature regime, $T \lesssim 10$ MeV, however, it increases with temperature. For comparison, in the same figure, the diquark gap in the model with $\mu_e = 0$ and $\mu_8 = 0$ is also shown (dash-dotted line). This latter has the standard BCS shape.

Another interesting thing regarding the temperature dependences in Fig. 10 appears in the intermediate temperature regime, $22.5 \lesssim T \lesssim 37$ MeV. By comparing the values of $\Delta(T)$ and $\delta\mu$ in this regime, we see that the g2SC phase is replaced by a “transitional” 2SC phase there. Indeed, the energy spectrum of the quasiparticles even at finite temperature is determined by the same relations in Eqs. (3.27) and (3.29) that we used at zero temperature. When $\Delta > \delta\mu$, the modes determined by Eq. (3.29) are gapped. Then, according to our standard classification, the ground state is the 2SC phase.

It is fair to say, of course, that the qualitative difference of the g2SC and 2SC phases is not so striking at finite temperature as it is at zero temperature. This difference is particularly negligible in the regime of interest where temperatures $22.5 \lesssim T \lesssim 37$ MeV are considerably larger than the actual value of the smaller gap, $\Delta - \delta\mu$. By increasing the value of the coupling constant slightly, however, the transitional 2SC phase can be made much stronger and the window of intermediate temperatures can become considerably wider. In either case, we find it rather unusual that the g2SC phase of neutral quark matter is replaced by a transitional 2SC phase at intermediate temperatures which, at higher temperatures, is replaced by the g2SC phase again.

It appears that the temperature dependence of the diquark gap is very sensitive to the choice of the diquark coupling strength $\eta = G_D/G_S$ in the model at hand. This is not surprising because the solution to the gap equation is very sensitive to this choice. The

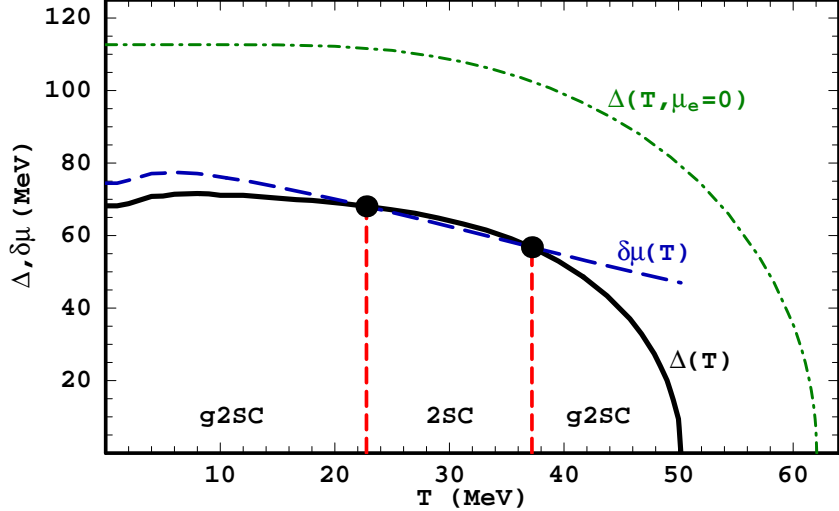


FIG. 10. The temperature dependence of the diquark gap (solid line) and the value of $\delta\mu \equiv \mu_e/2$ (dashed line) in neutral quark matter. For comparison, the diquark gap in the model with $\mu_e = 0$ and $\mu_8 = 0$ is also shown (dash-dotted line). The results are plotted for $\mu = 400$ MeV and $\eta = 0.75$.

resulting interplay of the solution for Δ with the condition of charge neutrality, however, is very interesting. This is demonstrated by the plot of the temperature dependence of the diquark gap calculated for several values of the diquark coupling in Fig. 11.

The most amazing are the results for weak coupling. It appears that the gap function could have sizable values at finite temperature even if it is exactly zero at zero temperature. This possibility comes about only because of the strong influence of the neutrality condition on the ground state preference in quark matter. Because of the thermal effects, the positive electric charge of the diquark condensate is easier to accommodate at finite temperature. This opens a possibility of the Cooper pairing that is forbidden at zero temperature.

We should mention that somewhat similar results for the temperature dependence of the gap were also obtained in Ref. [135] in a study of the asymmetric nuclear matter and in Ref. [136] in superfluidity. This behavior can be easily understood: When the coupling strength is relatively weak, at zero temperature, it is very difficult to form a pair for two fermions at largely separating sharp Fermi surfaces. However, when the temperature increases, the thermal excitations smooth the Fermi surfaces, thus offer the possibility for forming Cooper pairs. Of course, when the temperature is very high, the thermal excitations will eventually destroy the Cooper pairs.

Nonuniversal ratio T_c/Δ_0

In the preceding subsection, we saw that the temperature dependence of the gap in the g2SC phase is very different from the standard benchmark result in the BCS theory. One of the main properties of the BCS temperature dependence is a universal value of the ratio of the critical temperature T_c to the value of the gap at zero temperature Δ_0 , see Eq. (3.43). It is instructive, therefore, to calculate the same quantity in the g2SC phase of neutral quark matter.

Let us start from a simple exercise, and consider the results plotted in Fig. 10 more carefully. First of all, we find that $T_c^{2SC} \approx 62.06$ MeV and $\Delta_0^{2SC} = 109.4$ MeV when there is

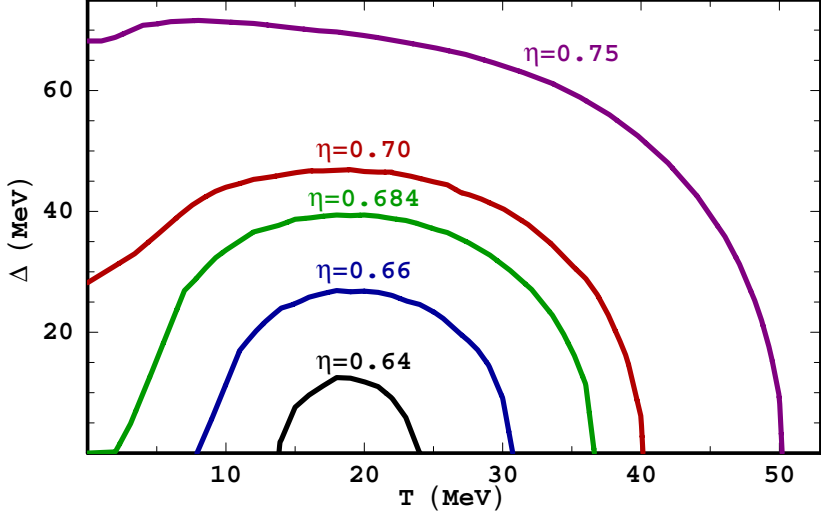


FIG. 11. The temperature dependence of the diquark gap in neutral quark matter calculated for several values of the diquark coupling strength $\eta = G_D/G_S$.

no mismatch parameters in the model (i.e., $\mu_e = 0$ and $\mu_8 = 0$ represented by dash-dotted line). It is not very surprising that the ratio of interest $r_{2SC} \approx 0.567$ is in agreement with the BCS result. Now, if we check the results for the gap function in the g2SC phase (solid line), we find that $T_c^{g2SC} \approx 50.2$ MeV and $\Delta_0^{g2SC} \approx 68.2$ MeV. Thus, the ratio is $r_{g2SC} \approx 0.7357$ which is considerably larger than the 2SC result.

It appears that the real situation is even more interesting. The result for the ratio $r_{g2SC} \approx 0.7357$ is not universal. In fact, its value depends very much on the diquark coupling constant and, moreover, it can even be arbitrarily large. This last statement may not be so unexpected if we recall the temperature dependences of the gap shown in Fig. 11.

The numerical results for the ratio of the critical temperature to the zero temperature gap in the g2SC case as a function of the diquark coupling strength $\eta = G_D/G_S$ are plotted in Fig. 12. The dependence is shown for the most interesting range of values of $\eta = G_D/G_S$, $0.68 \lesssim \eta \lesssim 0.81$, which allows the g2SC stable ground state at zero temperature. When the coupling gets weaker in this range, the zero temperature gap vanishes gradually. As we saw from Fig. 11, however, this does not mean that the critical temperature vanishes too. Therefore, the ratio of a finite value of T_c to the vanishing value of the gap can become arbitrarily large. In fact, it remains strictly infinite for a range of couplings.

E. Chromomagnetic instability in the g2SC phase

The g2SC phase has four gapless modes and two gapped modes, one may think that the low energy (large distance scale) properties in the g2SC phase should interpolate between those in the normal phase and those in the 2SC phase. However, its color screening properties do not fit this picture.

As we know, one of the most important properties of the ordinary superconductor is its Meissner effect, i.e., a superconductor expels the magnetic field, which was discovered by Meissner and Ochsenfeld in 1933 [35]. From theoretical point of view, the Messiner effect

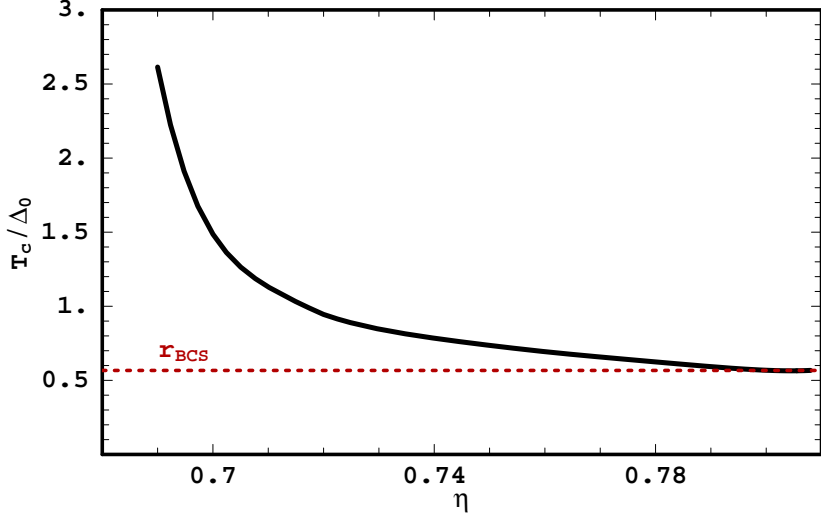


FIG. 12. The ratio of the critical temperature to the zero temperature gap in neutral quark matter as a function of the coupling strength $\eta = G_D/G_S$.

can be explained using the linear response theory. The induced current j_i^{ind} is related to the magnetic field A_j by $j_i^{ind} = \Pi_{ij} A^j$, where the response function Π_{ij} is the photon polarization tensor. The response function has two components, diamagnetic and paramagnetic part [137]. In the static and long-wavelength limit, for the normal metal, the paramagnetic component cancels exactly the diamagnetic component. While in the superconducting phase, the paramagnetic component is quenched by the energy gap and producing a net diamagnetic response. Thus the ordinary superconductor is a perfect diamagnet.

In color superconducting phases, the gluon self-energy (the response function to an external color field), has been investigated in the ideal 2SC phase [54] and in the CFL phase [59]. The results show that the gauge bosons connected with the broken generators obtain masses in these phases, which indicate the Meissner screening effect in these phases.

It is very interesting to know the chromomagnetic property in the g2SC phase. We studied the g2SC phase in the framework of the SU(2) NJL model, and the NJL model lacks gluons. As reflection of this, it possesses the global instead of gauged color symmetry. In addition, there appear five Nambu-Goldstone (NG) bosons in the ground state of the model when the color symmetry is broken. In QCD, there is no room for such NG bosons. However, the NJL model can be thought of as the low energy theory of QCD in which the gluons, as independent degrees of freedom, are integrated out. The gluons could be reintroduced back by gauging the color symmetry in the Lagrangian density of the NJL model, providing a semirigorous framework for studying the effect of the Cooper pairing on the physical properties of gluons.

The existence of the g2SC phase can be regarded as a physical and model independent result under the restriction of local charge neutrality condition, the order parameter for this phase is $\Delta < \delta\mu$. In Ref. [89], we calculated the gluon self-energy in the g2SC phase. It is found that, in this phase, the symmetry broken gauge bosons have imaginary Meissner screening masses, which is induced by the dominant paramagnetic contribution to the gluon self-energy. In condensed matter, this phenomenon is called the paramagnetic Meissner

effect(PME) [138], and has been observed in some high temperature superconductors and small superconductors.

Unavoidably, the imaginary Meissner screening mass indicates a chromomagnetic instability of the g2SC phase. There are several possibilities to resolve this instability. One is through a gluon condensate to stabilize the system, which may not change the structure of the g2SC phase. It is also possible that the instability drives a new stable ground state, which may have a rotational symmetry breaking like in Refs. [139,140], or even have an inhomogeneous phase structure, like a crystal [68–70] or a vortex [141] structure. In the future, one has to resolve this problem.

IV. THE MIXED PHASE AND NONSTRANGE HYBRID STAR

We have discussed the homogeneous two-flavor quark matter when charge neutrality conditions are satisfied locally, and found that the local charge neutrality conditions impose very strong constraints on determining the ground state of the system. In this section, we are going to discuss the mixed phase and the nonstrange hybrid star based on Ref. [142].

A. The mixed phase

When charge neutrality conditions are satisfied globally, one can construct a mixed phase [142–144]. Inside mixed phases, the charge neutrality is satisfied “on average” rather than locally. This means that different components of mixed phases may have nonzero densities of conserved charges, but the total charge of all components still vanishes. In this case, one says that the local charge neutrality condition is replaced by a global one. There are three possible components: (i) normal phase, (ii) 2SC phase, and (iii) g2SC phase.

The pressure of the main three phases of two-flavor quark matter as a function of the baryon and electric chemical potentials is shown in Fig. 13 at $\eta = 0.75$. In this figure, we also show the pressure of the neutral normal quark and gapless 2SC phases (two dark solid lines). The surface of the g2SC phase extends only over a finite range of the values of μ_e . It merges with the pressure surfaces of the normal quark phase (on the left) and with the ordinary 2SC phase (on the right).

It is interesting to notice that the three pressure surfaces in Fig. 13 form a characteristic swallowtail structure. As one could see, the appearance of this structure is directly related to the fact that the phase transition between color superconducting and normal quark matter, which is driven by changing parameter μ_e , is of first order. In fact, one should expect the appearance of a similar swallowtail structure also in a self-consistent description of the hadron-quark phase transition. Such a description, however, is possible.

From Fig. 13, one could see that the surfaces of normal and 2SC quark phases intersect along a common line. This means that the two phases have the same pressure along this line, and therefore could potentially co-exist. Moreover, as is easy to check, normal quark matter is negatively charged, while 2SC quark matter is positively charged on this line. This observation suggests that the appearance of the corresponding mixed phase is almost inevitable.

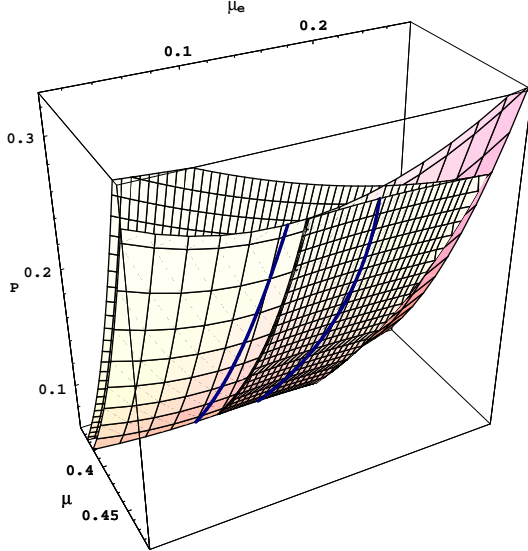


FIG. 13. At $\eta = 0.75$, pressure as a function of $\mu \equiv \mu_B/3$ and μ_e for the normal and color superconducting quark phases. The dark solid lines represent two locally neutral phases: (i) the neutral normal quark phase on the left, and (ii) the neutral gapless 2SC phase on the right. The appearance of the swallowtail structure is related to the first order type of the phase transition in quark matter.

Let us start by giving a brief introduction into the general method of constructing mixed phases by imposing the Gibbs conditions of equilibrium [145,146]. From the physical point of view, the Gibbs conditions enforce the mechanical as well as chemical equilibrium between different components of a mixed phase. This is achieved by requiring that the pressure of different components inside the mixed phase are equal, and that the chemical potentials (μ and μ_e) are the same across the whole mixed phase. For example, in relation to the mixed phase of normal and 2SC quark matter, these conditions read

$$P^{(NQ)}(\mu, \mu_e) = P^{(2SC)}(\mu, \mu_e), \quad (4.1)$$

$$\mu = \mu^{(NQ)} = \mu^{(2SC)}, \quad (4.2)$$

$$\mu_e = \mu_e^{(NQ)} = \mu_e^{(2SC)}. \quad (4.3)$$

It is easy to visualize these conditions by plotting the pressure as a function of chemical potentials (μ and μ_e) for both components of the mixed phase. This is shown in Fig. 14. As should be clear, the above Gibbs conditions are automatically satisfied along the intersection line of two pressure surfaces (dark solid line in Fig. 14).

Different components of the mixed phase occupy different volumes of space. To describe this quantitatively, we introduce the volume fraction of normal quark matter as follows: $\chi_{2SC}^{NQ} \equiv V_{NQ}/V$ (notation χ_B^A means volume fraction of phase A in a mixture with phase B). Then, the volume fraction of the 2SC phase is given by $\chi_{NQ}^{2SC} = (1 - \chi_{2SC}^{NQ})$. From the definition, it is clear that $0 \leq \chi_{2SC}^{NQ} \leq 1$.

The average electric charge density of the mixed phase is determined by the charge densities of its components taken in the proportion of the corresponding volume fractions. Thus,

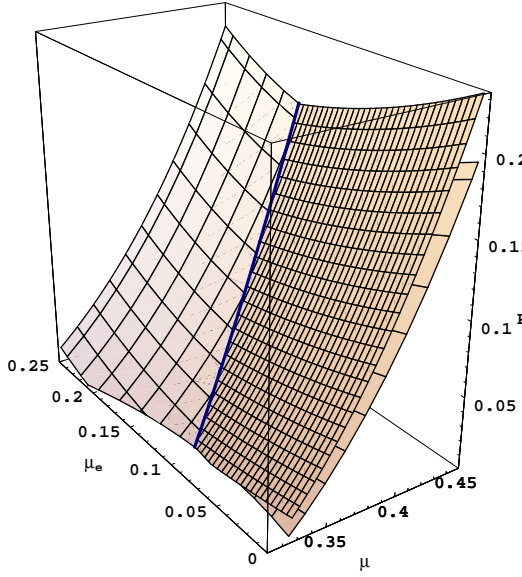


FIG. 14. At $\eta = 0.75$, pressure as a function of $\mu \equiv \mu_B/3$ and μ_e for the normal and color superconducting quark phases (the same as in Fig. 13, but from a different viewpoint). The dark solid line represents the mixed phase of negatively charged normal quark matter and positively charged 2SC matter.

$$n_e^{(MP)} = \chi_{2SC}^{NQ} n_e^{(NQ)}(\mu, \mu_e) + (1 - \chi_{2SC}^{NQ}) n_e^{(2SC)}(\mu, \mu_e). \quad (4.4)$$

If the charge densities of the two components have opposite signs, one can impose the global charge neutrality condition, $n_e^{(MP)} = 0$. Otherwise, a neutral mixed phase could not exist. In the case of quark matter, the charge density of the normal quark phase is negative, while the charge density of the 2SC phase is positive along the line of the Gibbs construction (dark solid line in Fig. 14). Therefore, a neutral mixed phase may exist. The volume fractions of its components are

$$\chi_{2SC}^{NQ} = \frac{n_e^{(2SC)}}{n_e^{(2SC)} - n_e^{(NQ)}}, \quad (4.5)$$

$$\chi_{NQ}^{2SC} \equiv 1 - \chi_{2SC}^{NQ} = \frac{n_e^{(NQ)}}{n_e^{(NQ)} - n_e^{(2SC)}}. \quad (4.6)$$

After the volume fractions have been determined from the condition of the global charge neutrality, we could also calculate the energy density of the corresponding mixed phase,

$$\varepsilon^{(MP)} = \chi_{2SC}^{NQ} \varepsilon^{(NQ)}(\mu, \mu_e) + (1 - \chi_{2SC}^{NQ}) \varepsilon^{(2SC)}(\mu, \mu_e). \quad (4.7)$$

This is essentially all that we need in order to construct the equation of state of the mixed phase.

So far, we were neglecting the effects of the Coulomb forces and the surface tension between different components of the mixed phase. In a real system, however, these are

important. In particular, the balance between the Coulomb forces and the surface tension determines the size and geometry of different components inside the mixed phase.

In our case, nearly equal volume fractions of the two quark phases are likely to form alternating layers (slabs) of matter. The energy cost per unit volume to produce such layers scales as $\sigma^{2/3}(n_e^{(2SC)} - n_e^{(NQ)})^{2/3}$ where σ is the surface tension [147]. Therefore, the quark mixed phase is a favorable phase of matter only if the surface tension is not too large. Our simple estimates show that $\sigma_{max} \leq 20$ MeV/fm². However, even for slightly larger values, $20 \leq \sigma \leq 50$ MeV/fm², the mixed phase is still possible, but its first appearance would occur at larger densities, $3\rho_0 \leq \rho_B \leq 5\rho_0$. The value of the maximum surface tension obtained here is comparable to the estimate in the case of the hadronic-CFL mixed phase obtained in Ref. [148]. The thickness of the layers scales as $\sigma^{1/3}(n_e^{(2SC)} - n_e^{(NQ)})^{-2/3}$ [147], and its typical value is of order 10 fm in the quark mixed phase. This is similar to the estimates in various hadron-quark and hadron-hadron mixed phases [147,148]. While the actual value of the surface tension in quark matter is not known, in this study we assume that it is not very large. Otherwise, the homogeneous gapless 2SC phase should be the most favorable phase of nonstrange quark matter [87].

Under the assumptions that the effect of Coulomb forces and the surface tension is small, the mixed phase of normal and 2SC quark matter is the most favorable neutral phase of matter in the model at hand with $\eta = 0.75$. This should be clear from observing the pressure surfaces in Figs. 13 and 14. For a given value of the baryon chemical potential $\mu = \mu_B/3$, the mixed phase is more favorable than the gapless 2SC phase, while the gapless 2SC phase is more favorable than the neutral normal quark phase.

B. Nonstrange hybrid star

In order to construct a neutron star, we need to know the equation of state from very low baryon density to very high baryon density. Unfortunately, currently there is no single model that can describe the whole bayron density regime very successfully. In the following, we use a QCD-motivated hadronic chiral $SU(3)_L \times SU(3)_R$ model in normal baryon density regime, and use the NJL model in the quark phase.

Hadronic matter

At densities around normal nuclear matter density $\rho_0 \approx 0.15$ fm⁻³, the description of baryonic matter in terms of quarks could hardly be adequate. At such low densities, quarks are confined inside hadrons. Thus, it is more natural to use an effective hadronic model.

We use a QCD-motivated hadronic chiral $SU(3)_L \times SU(3)_R$ model as an effective theory of strong interactions to describe the low density regime of the baryonic matter [149–151]. This model was found to describe reasonably well the hadronic masses of various $SU(3)$ multiplets, finite nuclei, hypernuclei, excited nuclear matter and neutron star properties [149–151]. The basic features of the chiral model are: (i) Lagrangian of the model is constructed in accordance with the nonlinear realization of the chiral $SU(3)_L \times SU(3)_R$ symmetry; (ii) heavy baryons and mesons get their masses as a result of spontaneous symmetry breaking; (iii) the masses of pseudoscalar mesons (pseudo-Nambu-Goldstone bosons) result from an explicit symmetry breaking; (iv) a QCD-motivated field that describes the gluon condensate (dilaton

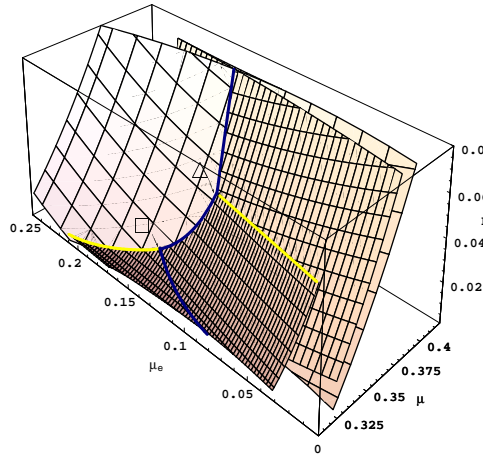


FIG. 15. Pressure as a function of $\mu \equiv \mu_B/3$ and μ_e for the hadronic phase (at the bottom), for the two-flavor color superconducting phase (on the right in front) and the normal phase of quark matter (on the left, and back on the right). The dark thick line follows the neutrality line in hadronic matter, and two mixed phases: (i) the mixed phase of hadronic and normal quark matter; and (ii) the mixed phase of normal and color superconducting quark matter.

field) is introduced.

The mixed phase of hadronic matter and quark matter

It is expected that the phase transition between the hadronic phase and the normal quark phase is a first order phase transition at zero temperature and finite baryon chemical potential. Then, the hadronic and quark phases could co-exist in a mixed phase [145,146]. This mixed phase should satisfy the Gibbs conditions of equilibrium which are similar to those discussed in the previous section, see Eqs. (4.1)–(4.3). The total energy density in the hadron-quark mixed phase is given by

$$\varepsilon^{(MP)} = \chi_H^{NQ} \epsilon^{(NQ)}(\mu, \mu_e) + (1 - \chi_H^{NQ}) \epsilon^{(H)}(\mu, \mu_e), \quad (4.8)$$

where χ_H^{NQ} denotes the volume fraction of normal quark matter inside a mixture with hadronic matter.

To visualize the Gibbs construction of the hadron-quark mixed phase, we plot the hadronic surface of the pressure along with the quark surfaces discussed in the previous section. Thus, Fig. 14 is replaced by Fig. 15. The new figure shows the surfaces of the pressure of the pure hadronic and quark phases as a function of their chemical potentials μ and μ_e . The intersection lines of different surfaces indicate all potentially viable mixed phase constructions. Although the Gibbs conditions are satisfied along all these lines, not

all of them could produce globally neutral phases (e.g., there are no neutral constructions along the light shaded solid lines in Fig. 15).

The dark solid line gives the complete, most favorable construction of globally neutral matter in general β -equilibrium. This line consists of three pieces. The lowest part of the curve (up to the point denoted by \square and $P \lesssim 10 \text{ MeV/fm}^3$) corresponds to the pure confined hadronic phase. Within this regime matter is mostly composed of neutrons with little fractions of protons and electrons to realize the charge neutrality and β -equilibrium. The hyperonic particles (Λ , Σ and Ξ) are not present in this lowest density regime. Such particles would appear in the hadronic phase at considerably higher values of pressure and density.

The mixed phase of hadronic and normal quark matter starts at the baryonic density $\rho_B \approx 1.49\rho_0$ which corresponds to the \square -point in Fig. 15. At this point the first bubbles of deconfined quark matter appear in the system. At the beginning of this hadron-quark mixed phase, the deconfined bubbles are small but highly negatively charged, whereas hadronic matter, in which the bubbles are embedded, is slightly positively charged. The global charge neutrality condition reads

$$n_e^{(MP)} \equiv \chi_H^{NQ} n_e^{(NQ)}(\mu, \mu_e) + (1 - \chi_H^{NQ}) n_e^{(H)}(\mu, \mu_e) = 0. \quad (4.9)$$

where $n_e^{(H)}$ and $n_e^{(NQ)}$ are the charge densities of hadronic and normal quark matter, respectively. This condition should be satisfied at each point along the middle part of the dark solid line (i.e., between the points denoted by \square and \triangle). With increasing density (from about $1.49\rho_0$ up to $2.56\rho_0$), the volume fraction of hadronic matter decreases (down to about 0.59), while the fraction of normal quark matter increases (up to about 0.41).

Equation of state

The equations of state for quark and hybrid matter are shown in Fig. 16. The first equation of state corresponds to globally neutral quark matter which is a mixture of the normal quark and 2SC phases. As for the equation of state of hybrid matter, it is constructed out of the equation of state of neutral hadronic matter and two Gibbs constructions in accordance with Fig. 15. As before, the points that indicate the beginning of two different mixed phases are denoted by \square and \triangle in Fig. 16.

Mass-radius relation for hybrid star

The mass-radius relations for hybrid and pure quark stars are shown in Fig. 17. As one would expect, the pure quark stars composed of the mixed phase have much smaller radii and the value of their maximum mass is slightly smaller, see Fig. 17. Our results for pure quark stars are comparable to those in Refs. [122,152]. The difference between hybrid and pure quark stars is mostly due to the low density part of the equation of state. This is also evident from the qualitative difference in the dependence of the radius as a function of mass for the hybrid and quark stars with low masses. The corresponding hybrid stars are large because of a sizable low density hadronic layer, while the quark stars are small because that have no such layers.

Here we use a two-flavor version of the NJL model to describe the deconfined phase. However, the three-flavor extension of the NJL model in Ref. [120] suggests that strange

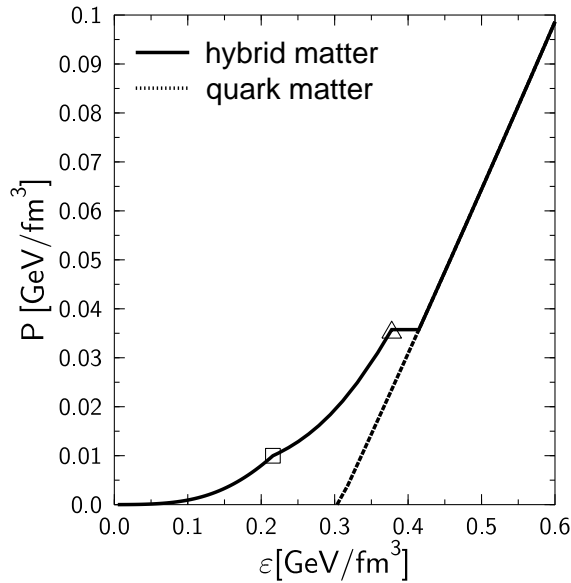


FIG. 16. The equation of state for globally neutral hybrid matter (solid line) and globally neutral quark matter (dashed line). The points of the beginning of the two mixed phases are denoted by \square and \triangle .

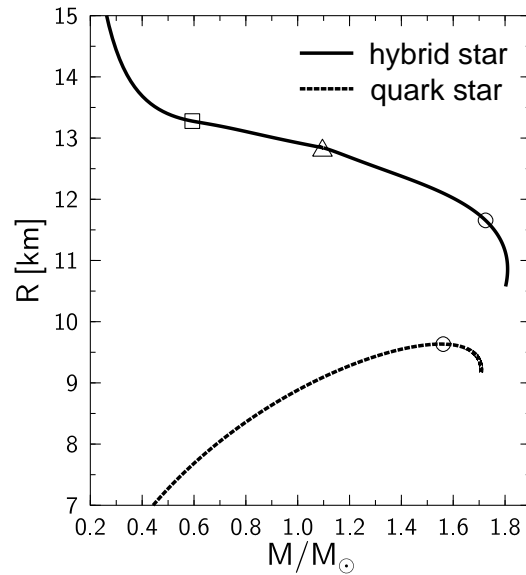


FIG. 17. The mass-radius relations for hybrid stars (solid line) and quark stars (dashed line).

quarks might be present in matter above a critical density of about $5\rho_0$. For the consideration of strange quark star in the framework of the NJL model, please see Ref. [153].

V. CONCLUSION AND OUTLOOK

This article focuses on the two-flavor color superconducting phase at moderate baryon density.

In order to simultaneously investigate the chiral phase transition and the color superconducting phase transition, the Nambu-Gorkov formalism has been extended to treat the quark-antiquark and diquark condensates on an equal footing, and the competition between the chiral and diquark condensates has been investigated.

Dense u, d quark matter under local and global charge neutrality conditions in β -equilibrium has been discussed in detail. Under the local charge neutrality condition, the homogeneous neutral ground state is sensitive to the coupling constant in the diquark channel, it will be in the regular 2SC phase when the diquark coupling is strong, in the normal phase when the diquark coupling is weak, and in the g2SC phase in the case of intermediate diquark coupling. The low energy quasi-particle spectrum of the g2SC phase contains four gapless modes and only two gapped modes. In the intermediate diquark coupling regime, under global charge neutrality condition, assuming that the effect of Coulomb forces and the surface tension is small, one can construct a mixed phase composed of a positive charged 2SC phase and a negative charged normal quark phase. It will be valuable to compare the homogeneous g2SC phase and the mixed phase, and give a clear answer to which phase is preferable.

Even though the regime of the diquark coupling strength for the existence of the g2SC phase is rather narrow, i.e., $0.7 \lesssim \eta \lesssim 0.8$, it is noticed that the value $\eta = 0.75$ from Fierz transformation and also the value $\eta \simeq 2.26/3$ from fitting the baryon vacuum mass, are inside this regime. The g2SC has rather unusual properties at zero as well as at finite temperature, and its chromomagnetic properties are extremely surprising. The paramagnetic Meissner effect indicates a chromomagnetic instability in the g2SC phase. In the near future, we need to resolve the problem of the chromomagnetic instability in the g2SC phase, and to investigate whether the chromomagnetic instability will drive a new inhomogeneous structure.

In this article, I only discussed the two-flavor quark system. In the moderate baryon density regime $\mu \simeq 500\text{MeV}$, the strange quark may appear in the system. The cold dense three-flavor quark system has a more complicated and more interesting phase structure. In different conditions, the three-flavor quark system can be in one of the phases of CFL, CFL+K, CFL+ η , gCFL, and dSC [78,79,86,90–94]. It is, of course, very interesting and also challenging to investigate all these phases in one self-consistent framework. For the charge neutral gCFL phase, it is very attractive to know whether there is chromomagnetic instability.

In our calculations, we used the mean-field approximation. It is very interesting to see how the diquark fluctuation will affect the results. It should be noticed that till now, we are using the BCS scenario even in the intermediate baryon density regime. From the experience in condensed matter, the BCS scenario only works when the attractive interaction is very

weak, where the Cooper pairs are loosely bound states. While with the increasing of the coupling strength, the Cooper pairs become tightly bounded, the fluctuation from the Cooper pairs cannot be neglected. In the strong coupling case, the Cooper pairs become real bound states in the coordinates space, and a Fermion system transfers to a boson system. The boson system may experience the Bose-Einstein condensation (BEC). This is the basic idea of the crossover from BCS to BEC [154,155]. The fluctuation of the gauge fields as well as of the diquark were investigated in Refs. [156,157], and it will be very interesting to see how the Cooper pair structure [158] changes when fluctuations are considered. In addition to the diquark fluctuation, the quark-antiquark fluctuation may also need to be considered in the intermediate baryon density regime. It was found in Ref. [159] that the quark-antiquark fluctuation has significant influence on the chiral phase transition. When the quark-antiquark fluctuation is considered self-consistently [160], the critical baryon density for the chiral phase transition becomes much larger than that in the mean-field approximation.

The most interesting thing in the field of color superconductivity, of course, is to look for this phase in the nature or to create this phase in the laboratory. There are already some work to find the possibility of the existence of the color superconducting phase inside the neutron star, like the mass-radius relation [122,142,152,153] and the cooling history [161]. The energy release from a hadronic star to a color superconducting star may relate to the supernovae or the gamma-ray burst [162]. About the possibility of creation color superconductivity in heavy-ion collisions, the work is in progress [163]. Nevertheless, we are just at the very beginning of this field, and there is still a long way to go.

VI. ACKNOWLEDGEMENTS

I thank Prof. Wei-qin Chao and Prof. Peng-fei Zhuang for their continuous encouragement during my research work in this field. Most part of the research work in Sec. III and Sec. IV of this paper have been done in Frankfurt. I am grateful to my host professor, Prof. Horst Stoecker, for his hospitality and for giving me freedom to do what I like. I thank Prof. Dirk Rischke, who motivated our study on the thermal stability of the g2SC phase. I thank all the members in the “Frankfurt-Darmstadt Color Superconductivity Group”. I give my special thanks to Dr. Igor Shovkovy for reading this manuscript very carefully and for our fruitful and happy collaboration. During the two-year collaboration, we shared all the exciting discoveries, especially the g2SC phase and its unusual properties.

Finally, I acknowledge the financial support from the Alexander von Humboldt-Foundation, and from the NSFC under Grant Nos. 10105005, 10135030.

APPENDIX A: FIERZ TRANSFORMATION

Color-current interaction has the form of

$$\mathcal{L}_{int}^c = -G_c \sum_{a=1}^8 [\bar{\psi}_{\alpha r}^i(\gamma_\mu)_{rs}(t^a)_{\alpha\beta} \delta^{ij} \psi_{\beta s}^j] [\bar{\psi}_{\gamma t}^k(\gamma^\mu)_{tu}(t^a)_{\gamma\delta} \delta^{kl} \psi_{\delta u}^l], \quad (\text{A1})$$

where $t^a = (\lambda^a)_C/2$ are the SU(3) color generators with $tr(t^a t^b) = \delta_{ab}/2$, $\alpha, \beta, \gamma, \delta$ are color indices acting on color space, i, j, k, l are flavor indices acting on flavor space, and r, s, t, u are spinor indices acting on Dirac space.

Fierz transformation in the Dirac space

Defining $S = 1 \otimes 1$, $V = \gamma_\mu \otimes \gamma^\mu$, $T = \sigma_{\mu\nu} \otimes \sigma^{\mu\nu}$, $A = \gamma_\mu \gamma_5 \otimes \gamma^\mu \gamma_5$, $P = \gamma_5 \otimes \gamma_5$, the exchange of the spinor indices s and u or r and t , can be represented as

$$\Gamma_{rs,tu}^i = \sum_j C_{ij} \Gamma_{ru,ts}^j, \quad (\text{A2})$$

where $\Gamma^i \in (S, V, T, A, P)$, and

$$\sum_j C_{ij} C_{jk} = \delta_{ik}. \quad (\text{A3})$$

The explicit expression for the above equation reads

$$\begin{pmatrix} S \\ V \\ T \\ A \\ P \end{pmatrix}' = \begin{pmatrix} -1/4 & -1/4 & -1/8 & 1/4 & -1/4 \\ -1 & 1/2 & 0 & 1/2 & 1 \\ -3 & 0 & 1/2 & 0 & -3 \\ 1 & 1/2 & 0 & 1/2 & -1 \\ -1/4 & 1/4 & -1/8 & -1/4 & -1/4 \end{pmatrix} \begin{pmatrix} S \\ V \\ T \\ A \\ P \end{pmatrix}, \quad (\text{A4})$$

In the following, we only need the transformation of V , i.e.,

$$\begin{aligned} (\gamma_\mu \otimes \gamma^\mu)_{rs,tu} &= -(\mathbf{1} \otimes \mathbf{1} + i\gamma_5 \otimes i\gamma_5)_{ru,ts} \\ &\quad + \frac{1}{2}(\gamma_\mu \otimes \gamma^\mu + \gamma_\mu \gamma_5 \otimes \gamma^\mu \gamma_5)_{ru,ts} \\ &= -(K_a \otimes K^a)_{ru,ts}, \end{aligned} \quad (\text{A5})$$

where $K_a = \{\mathbf{1}, i\gamma_5, \frac{i}{\sqrt{2}}\gamma_\mu, \frac{i}{\sqrt{2}}\gamma_\mu \gamma_5\}$, from which we can see that the contribution of the tensor part is zero, and thus the chiral symmetry is preserved.

For diquarks, we have

$$\begin{aligned} (\gamma_\mu)_{rs}(\gamma^\mu)_{tu} &= (\gamma_\mu)_{rs}((\gamma^\mu)^T)_{ut} \\ &= (\gamma_\mu)_{rs}(C\gamma^\mu C)_{ut} \\ &= C_{ua}C_{bt}(\gamma_\mu)_{rs}(\gamma^\mu)_{ab} \\ &= -(K_a C \otimes C K^a)_{rt,us}, \end{aligned} \quad (\text{A6})$$

where $C = i\gamma^2\gamma^0$ is the charge conjugation matrix.

1. Fierz transformation in the quark-antiquark sector

We will use the Fierz transformation in the color, flavor and Dirac spaces respectively.

Fierz identity in the color space

The standard identity

$$t_{\alpha\beta}^c t_{\gamma\delta}^c = \frac{1}{2} \left(1 - \frac{1}{N_c^2}\right) \delta_{\alpha\delta} \delta_{\gamma\beta} - \frac{1}{N_c} t_{\alpha\delta}^c t_{\gamma\beta}^c, \quad (\text{A7})$$

gives both the color singlet and color octet terms.

Fierz identity in the flavor space

Rewrite

$$\delta_{ij} \delta_{kl} = \sum_e (G^e)_{il} (G^e)_{kj}, \quad (\text{A8})$$

where G^e has been ordered in the way flavor singlet + octet, with

$$\{G^e\} = \left(\frac{1}{\sqrt{3}} \mathbf{1} \equiv \frac{(\lambda^0)_F}{\sqrt{2}}, \frac{(\lambda^a)_F}{\sqrt{2}} \right), a = 1, \dots, 8. \quad (\text{A9})$$

Color singlet part

Using Eqs. (A5), (A7) and (A8), we can get the color singlet part of the Lagrange Eq. (A1),

$$\begin{aligned} \mathcal{L}_{int}^{1c} = & \frac{8}{9} G_c \sum_{a=0}^8 [(\bar{\psi} \frac{\lambda_F^a}{2} \psi)^2 + (\bar{\psi} i \gamma_5 \frac{\lambda_F^a}{2} \psi)^2] \\ & - \frac{4}{9} G_c \sum_{a=0}^8 [(\bar{\psi} \gamma_\mu \frac{\lambda_F^a}{2} \psi)^2 + (\bar{\psi} \gamma_\mu \gamma_5 \frac{\lambda_F^a}{2} \psi)^2]. \end{aligned} \quad (\text{A10})$$

2. Fierz transformation in the diquark sector

Fierz identity in the color space

$$t_{\alpha\beta}^c t_{\gamma\delta}^c = \frac{2}{N_c} \sum_S t_{\alpha\gamma}^S t_{\delta\beta}^S - \frac{4}{N_c} \sum_A t_{\alpha\gamma}^A t_{\delta\beta}^A, \quad (\text{A11})$$

where $S \in \{0, 1, 3, 4, 6, 8\}$ denotes the symmetric and $A \in \{2, 5, 7\}$ the antisymmetric Gell-Mann matrices.

The above identity is decomposed in the way of $6_c + \bar{3}_c$, which shows that the interaction in the 6_c channel is opposite to that in the $\bar{3}_c$ channel. There is another decomposition in the way of $1_c + \bar{3}_c$, i.e.,

$$t_{\alpha\beta}^c t_{\gamma\delta}^c = \frac{1}{2} \left(1 - \frac{1}{N_c}\right) \delta_{\alpha\delta} \delta_{\gamma\beta} + \frac{1}{2N_c} \epsilon_{\alpha\gamma}^\rho \epsilon_{\delta\beta}^\rho, \quad (\text{A12})$$

which shows that the interaction in the color antitriplet channel has the same symbol as that in the singlet channel. The interaction in the color singlet channel 1_c is attractive, so is the color antitriplet channel $\bar{3}_c$. The former is responsible for the bound state of meson, the latter is responsible for the bound state of baryon, as well as the quark-quark Cooper pairing at high baryon density. The ratio of the magnitude of the coupling constant in $\bar{3}_c$ channel and 1_c channel is $1/2$ from Eq. (A12).

Fierz identity in the flavor space

$$\delta_{ij} \delta_{kl} = \sum_e (G^e)_{ik} (G^e)_{lj}, \quad (\text{A13})$$

where

$$\{G^e\} = \{G_A^e, G_S^e\} = \left\{ \frac{\lambda_F^2}{\sqrt{2}}, \frac{\lambda_F^5}{\sqrt{2}}, \frac{\lambda_F^7}{\sqrt{2}}; \frac{1}{\sqrt{3}} \mathbf{1} \equiv \frac{\lambda_F^0}{\sqrt{2}}, \frac{\lambda_F^1}{\sqrt{2}}, \frac{\lambda_F^3}{\sqrt{2}}, \frac{\lambda_F^4}{\sqrt{2}}, \frac{\lambda_F^6}{\sqrt{2}}, \frac{\lambda_F^8}{\sqrt{2}} \right\}. \quad (\text{A14})$$

where $S \in \{0, 1, 3, 4, 6, 8\}$ denotes the symmetric and $A \in \{2, 5, 7\}$ the antisymmetric Gell-Mann matrices.

Color anti-triplet part

First, using Eqs. (A6), we have

$$\begin{aligned} & [\bar{\psi}_r (\gamma_\mu)_{rs} \psi_s] [\bar{\psi}_t (\gamma^\mu)_{tu} \psi_u] \\ &= [\bar{\psi}_r (K_a C)_{rt} \bar{\psi}_t] [\psi_s (C K^a)_{us} \psi_u] \\ &= [\bar{\psi}_r (K_a C)_{rt} \bar{\psi}_t] [\psi_s (C K^a)_{us} \psi_u] \\ &= [\bar{\psi} K_a C \bar{\psi}^T] [\psi^T C K^a \psi]. \end{aligned} \quad (\text{A15})$$

Then, using Eq. (A12) the color anti-triplet part can be expressed as

$$\begin{aligned} & [\bar{\psi}_{\alpha r} (\gamma_\mu)_{rs} (t^a)_{\alpha\beta} \psi_{\beta s} [\bar{\psi}_{\gamma t} (\gamma^\mu)_{tu} (t^a)_{\gamma\delta} \psi_{\delta u}] \\ &= -\frac{1}{3} [\bar{\psi} K_a C \frac{i\epsilon^\rho}{\sqrt{2}} \bar{\psi}^T] [\psi^T C K^a \frac{i\epsilon^\rho}{\sqrt{2}} \psi]. \end{aligned} \quad (\text{A16})$$

At last, the flavor structure is determined by the Pauli principle. A color triplet diquark state is antisymmetric under the exchange of colors, due to the Pauli principle, the matrices $C K^a \lambda_F$ must be totally symmetric. Thus the axial-vector and scalar diquark currents transform according to antisymmetric flavor $\bar{3}$ representation, whereas the scalar-, pseudoscalar- and vector-diquarks are necessarily flavor sextets.

APPENDIX B: CHARGE CONJUGATION

Charge conjugation is conventionally defined to take a fermion with a given spin orientation into an antifermion with the same spin orientation.

The charge-conjugated field ψ^C is defined by

$$\begin{aligned}\psi^C(x) &= C\bar{\psi}^T(x), \bar{\psi}^C(x) = \psi^T C, \\ \psi(x) &= C\bar{\psi}^{CT}(x), \bar{\psi}(x) = \psi^{CT}(x)C,\end{aligned}\tag{B1}$$

where $C = i\gamma^2\gamma^0$ is the charge-conjugation matrix in the Dirac representation,

$$C = -C^{-1} = -C^T = -C^\dagger,\tag{B2}$$

and

$$C\gamma^\mu C^{-1} = -(\gamma^\mu)^T.\tag{B3}$$

The charge conjugation of bilinears is a little tricky, and it helps to write in spinor indices. For the scalar,

$$\begin{aligned}\bar{\psi}^C \psi^C &= \bar{\psi}_\alpha^C \psi_\alpha^C \\ &= (\psi^T C)_\alpha (C\bar{\psi}^T)_\alpha \\ &= \psi_\lambda C_{\lambda\alpha} C_{\alpha\lambda'} \bar{\psi}_{\lambda'} \\ &= \bar{\psi}\psi.\end{aligned}\tag{B4}$$

In the last step, the fermion anticommutation and $CC = -1$ have been used.

For the vector,

$$\begin{aligned}\bar{\psi}^C \gamma^\mu \psi^C &= \bar{\psi}_\alpha^C (\gamma^\mu)_{\alpha\beta} \psi_\beta^C \\ &= (\psi^T C)_\alpha (\gamma^\mu)_{\alpha\beta} (C\bar{\psi}^T)_\beta \\ &= \psi_\lambda C_{\lambda\alpha} (\gamma^\mu)_{\alpha\beta} C_{\beta\lambda'} \bar{\psi}_{\lambda'} \\ &= \psi_\lambda (\gamma^\mu)_{\lambda\lambda'}^T \bar{\psi}_{\lambda'} \\ &= -\bar{\psi}_{\lambda'} (\gamma^\mu)_{\lambda'\lambda} \psi_\lambda \\ &= -\bar{\psi} \gamma^\mu \psi.\end{aligned}\tag{B5}$$

For the kinetic term,

$$\bar{\psi}^C \gamma^\mu \partial_\mu \psi^C = -(\partial_\mu \bar{\psi}) \gamma^\mu \psi,\tag{B6}$$

using

$$\partial_\mu (\bar{\psi} \gamma^\mu \psi) = (\partial_\mu \bar{\psi}) \gamma^\mu \psi + \bar{\psi} \gamma^\mu (\partial_\mu \psi),\tag{B7}$$

and the vector current conservation, we have

$$\bar{\psi}^C \gamma^\mu \partial_\mu \psi^C = \bar{\psi} \gamma^\mu \partial_\mu \psi.\tag{B8}$$

REFERENCES

- [1] D.J. Gross and F. Wilczek, Phys. Rev. Lett. **30** (1973) 1343; H.D. Politzer, Phys. Rev. Lett. **30** (1973) 1346.
- [2] E. Klempt, hep-ph/0404270.
- [3] T. Nakano *et al.* [LEPS Collaboration], Phys. Rev. Lett. **91**, 012002 (2003).
- [4] V. Kubarovskiy *et al.* [CLAS Collaboration], Phys. Rev. Lett. **92**, 032001 (2004); [Erratum-*ibid.* **92**, 049902 (2004)].
- [5] D. Diakonov, V. Petrov and M.V. Polyakov, Z. Phys. A **359**, 305 (1997).
- [6] R.L. Jaffe and F. Wilczek, Phys. Rev. Lett. **91**, 232003 (2003).
- [7] E. Shuryak and I. Zahed, Phys. Lett. B **589**, 21 (2004).
- [8] S.L. Zhu, Phys. Rev. Lett. **91**, 232002 (2003); S.L. Zhu, hep-ph/0406204.
- [9] T.D. Lee and G.C. Wick, Phys. Rev. D **9**, 2291 (1974).
- [10] J.C. Collins and M.J. Perry, Phys. Rev. Lett. **34**, 1353 (1975).
- [11] G. Baym and S.A. Chin, Phys. Lett. B **62**, 241 (1976).
- [12] E.V. Shuryak, Phys. Lett. B **78**, 150 (1978).
- [13] F. Karsch and E. Laermann, Phys. Rev. D **50**, 6954 (1994); F. Karsch, Nucl. Phys. A **698**, 199 (2002).
- [14] T. Hatsuda and T. Kunihiro, Phys. Rev. Lett. **55**, 158 (1985).
- [15] E.V. Shuryak and I. Zahed, hep-ph/0307267; E. Shuryak, Prog. Part. Nucl. Phys. **53**, 273 (2004); E.V. Shuryak and I. Zahed, hep-ph/0403127; E.V. Shuryak, hep-ph/0405066.
- [16] D.H. Rischke, Prog. Part. Nucl. Phys. **52**, 197 (2004).
- [17] M. Gyulassy and L. McLerran, nucl-th/0405013.
- [18] P. Jacobs and X.N. Wang, hep-ph/0405125.
- [19] U.W. Heinz, hep-ph/0407360.
- [20] H.R. Jaqaman, A.Z. Mekjian, and L. Zamick, Phys. Rev. C **29**, 2067(1984); R.K. Su, F.M. Lin Phys. Rev. C **39**, 2438(1989).
- [21] U.W. Heinz, P. R. Subramanian, H. Stocker and W. Greiner, J. Phys. G **12**, 1237 (1986).
- [22] S.C. Frautschi, Asymptotic freedom and color superconductivity in dense quark matter, Proc.of the Workshop on Hadronic Matter at Extreme Energy Density, N. Cabibbo (Editor), Erice, Italy (1978).
- [23] F. Barrois, Nucl. Phys. **B129** (1977),390.
- [24] J. Bardeen, L.N. Cooper, J.R. Schrieffer *Phys. Rev.* 106:162 (1957); *Phys. Rev.* 108:1175 (1957).
- [25] D. Bailin and A. Love, Phys. Rep. **107**, 325(1984).
- [26] R. Rapp, T. Schäfer,E.V. Shuryak and M. Velkovsky, Phys.Rev.Lett.**81**,53(1998); M. Alford, K. Rajagopal and F. Wilczek, Phys.Lett.**B 422**,247(1998).
- [27] K. Rajagopal and F. Wilczek, hep-ph/0011333.
- [28] D.K. Hong, Acta Phys. Polon. B **32**, 1253 (2001).
- [29] M. Alford, Ann. Rev. Nucl. Part. Sci. **51**, 131 (2001).
- [30] G. Nardulli, Riv. Nuovo Cim. **25N3**, 1 (2002).
- [31] T. Schäfer, hep-ph/0304281.
- [32] M. Buballa, hep-ph/0402234.

- [33] H.C. Ren, hep-ph/0404074.
- [34] L.N. Cooper, Phys. Rev. **104**, 1189 (1956).
- [35] W. Meissner and R. Ochsenfeld, Naturwiss. **21**, 787 (1933).
- [36] D.T. Son, Phys. Rev. D **59**, 094019 (1999).
- [37] T. Schafer and F. Wilczek, Phys. Rev. D **60**, 114033 (1999).
- [38] R.D. Pisarski and D.H. Rischke, Phys. Rev. D **61**, 074017 (2000).
- [39] R.D. Pisarski and D.H. Rischke, Phys. Rev. D **61**, 051501 (2000).
- [40] D.K. Hong, Phys. Lett. B **473**, 118 (2000).
- [41] D.K. Hong, V.A. Miransky, I.A. Shovkovy and L.C.R. Wijewardhana, Phys. Rev. D **61**, 056001 (2000); [Erratum-ibid. D **62**, 059903 (2000)].
- [42] W.E. Brown, J.T. Liu and H.C. Ren, Phys. Rev. D **61**, 114012 (2000); W.E. Brown, J.T. Liu and H.C. Ren, Phys. Rev. D **62**, 054016 (2000); W.E. Brown, J.T. Liu and H.C. Ren, Phys. Rev. D **62**, 054013 (2000).
- [43] C. Manuel, Phys. Rev. D **62**, 114008 (2000).
- [44] R. Rapp, T. Schafer, E.V. Shuryak and M. Velkovsky, Annals Phys. **280**, 35 (2000).
- [45] J. Berges and K. Rajagopal, Nucl. Phys. B **538**, 215 (1999).
- [46] G.W. Carter and D. Diakonov, Phys. Rev. D **60**, 016004 (1999).
- [47] T.M. Schwarz, S.P. Klevansky and G. Papp, Phys. Rev. C **60**, 055205 (1999).
- [48] R. Nebauer and J. Aichelin, Phys. Rev. C **65**, 045204 (2002)
- [49] M. Buballa, J. Hosek and M. Oertel, Phys. Rev. D **65**, 014018 (2002); M. Buballa and M. Oertel, Nucl. Phys. A **703**, 770 (2002).
- [50] D. Ebert, K.G. Klimenko and H. Toki, Phys. Rev. D **64**, 014038 (2001); D. Ebert, V.V. Khudyakov, V.C. Zhukovsky and K.G. Klimenko, Phys. Rev. D **65**, 054024 (2002).
- [51] M. Huang, P.F. Zhuang and W.Q. Chao, Phys. Rev. D **65**, 076012 (2002).
- [52] T. Schafer and F. Wilczek, Phys. Lett. B **450**, 325 (1999).
- [53] N.J. Evans, S.D.H. Hsu and M. Schwetz, Nucl. Phys. B **551**, 275 (1999); N.J. Evans, S.D.H. Hsu and M. Schwetz, Phys. Lett. B **449**, 281 (1999); S.D.H. Hsu and M. Schwetz, Nucl. Phys. B **572**, 211 (2000).
- [54] D.H. Rischke, Phys. Rev. D **62**, 034007 (2000); D.H. Rischke and I.A. Shovkovy, Phys. Rev. D **66**, 054019 (2002).
- [55] M.G. Alford, K. Rajagopal and F. Wilczek, Nucl. Phys. **B537**, 443 (1999).
- [56] T. Schafer, Nucl. Phys. B **575**, 269 (2000).
- [57] N.J. Evans, J. Hormuzdiar, S.D.H. Hsu and M. Schwetz, Nucl. Phys. B **581**, 391 (2000).
- [58] I.A. Shovkovy and L.C.R. Wijewardhana, Phys. Lett. B **470**, 189 (1999).
- [59] D.H. Rischke, Phys. Rev. D **62**, 054017 (2000).
- [60] R. Casalbuoni and R. Gatto, Phys. Lett. B **464**, 111 (1999).
- [61] D. T. Son and M. A. Stephanov, Phys. Rev. D **61**, 074012 (2000); [Erratum-ibid. Phys. Rev. D **62**, 059902 (2000)].
- [62] T. Schafer and F. Wilczek, Phys. Rev. Lett. **82**, 3956 (1999).
- [63] T. Schafer, Phys. Rev. D **62**, 094007 (2000).
- [64] M. Buballa, J. Hosek and M. Oertel, Phys. Rev. Lett. **90**, 182002 (2003).
- [65] A. Schmitt, Q. Wang and D.H. Rischke, Phys. Rev. D **66**, 114010 (2002).
- [66] A. Schmitt, Q. Wang and D.H. Rischke, Phys. Rev. Lett. **91**, 242301 (2003); A. Schmitt, Q. Wang and D.H. Rischke, Phys. Rev. D **69**, 094017 (2004).

- [67] A. Schmitt, nucl-th/0405076.
- [68] A.I. Larkin, YuN. Ovchinnikov, *Zh. Eksp. Teor. Fiz.* **47** (1964), 1136; translation: *Sov. Phys. JETP* **20** (1962), 762.
- [69] P. Fulde, R.A. Ferrell, *Phys. Rev.* **135**, A550 (1964).
- [70] M.G. Alford, J.A. Bowers and K. Rajagopal, *Phys. Rev. D* **63**, 074016 (2001).
- [71] J.A. Bowers, J. Kundu, K. Rajagopal and E. Shuster, *Phys. Rev. D* **64**, 014024 (2001).
- [72] A.K. Leibovich, K. Rajagopal and E. Shuster, *Phys. Rev. D* **64**, 094005 (2001).
- [73] J. Kundu and K. Rajagopal, *Phys. Rev. D* **65**, 094022 (2002).
- [74] J.A. Bowers and K. Rajagopal, *Phys. Rev. D* **66**, 065002 (2002).
- [75] J.A. Bowers, hep-ph/0305301.
- [76] I. Giannakis, J.T. Liu and H.C. Ren, *Phys. Rev. D* **66**, 031501 (2002).
- [77] R. Casalbuoni and G. Nardulli, *Rev. Mod. Phys.* **76**, 263 (2004); R. Casalbuoni, M. Ciminale, M. Mannarelli, G. Nardulli, M. Ruggieri and R. Gatto, hep-ph/0404090; R. Casalbuoni, R. Gatto, M. Mannarelli, G. Nardulli and M. Ruggieri, hep-ph/0407210.
- [78] T. Schafer, *Phys. Rev. Lett.* **85**, 5531 (2000); P.F. Bedaque and T. Schafer, *Nucl. Phys. A* **697**, 802 (2002).
- [79] D.B. Kaplan and S. Reddy, *Phys. Rev. D* **65**, 054042 (2002).
- [80] T. Schafer, D.T. Son, M.A. Stephanov, D. Toublan and J.J.M. Verbaarschot, *Phys. Lett. B* **522**, 67 (2001).
- [81] V.A. Miransky and I.A. Shovkovy, *Phys. Rev. Lett.* **88**, 111601 (2002).
- [82] M. Rho, A. Wirzba and I. Zahed, *Phys. Lett. B* **473**, 126 (2000);
- [83] D.K. Hong, T. Lee and D.P. Min, *Phys. Lett. B* **477**, 137 (2000).
- [84] C. Manuel and M.H.G. Tytgat, *Phys. Lett. B* **479**, 190 (2000).
- [85] T. Schafer, *Phys. Rev. D* **65**, 074006 (2002).
- [86] A. Kryjevski, D.B. Kaplan and T. Schafer, hep-ph/0404290.
- [87] I. Shovkovy and M. Huang, *Phys. Lett. B* **564**, 205 (2003).
- [88] M. Huang and I. Shovkovy, *Nucl. Phys. A* **729**, 835 (2003).
- [89] M. Huang and I.A. Shovkovy, hep-ph/0407049, to appear in PRD; M. Huang and I.A. Shovkovy, hep-ph/0408268.
- [90] M. Alford, C. Kouvaris and K. Rajagopal, *Phys. Rev. Lett.* **92**, 222001 (2004); M. Alford, C. Kouvaris and K. Rajagopal, hep-ph/0406137.
- [91] K. Iida, T. Matsuura, M. Tachibana and T. Hatsuda, hep-ph/0312363.
- [92] S.B. Ruster, I.A. Shovkovy and D.H. Rischke, *Nucl. Phys. A* **743**, 127 (2004).
- [93] K. Fukushima, C. Kouvaris and K. Rajagopal, hep-ph/0408322.
- [94] A. Kryjevski and T. Schaefer, hep-ph/0407329.
- [95] R.D. Pisarski and D.H. Rischke, *Phys. Rev. D* **60**, 094013 (1999).
- [96] M. Rho, E.V. Shuryak, A. Wirzba and I. Zahed, *Nucl. Phys. A* **676**, 273 (2000).
- [97] M. Huang, P.F. Zhuang, W.Q. Chao, *Chin. Phys. Lett.* **19** (2002) 644; hep-ph/0110046.
- [98] H. Mishra and J. C. Parikh, *Nucl. Phys. A* **679**, 597 (2001).
- [99] M. Kitazawa, T. Koide, T. Kunihiro and Y. Nemoto, *Prog. Theor. Phys.* **108**, 929 (2002).
- [100] Y. Nishida, K. Fukushima and T. Hatsuda, hep-ph/0306066.
- [101] B. Vanderheyden and A.D. Jackson, *Phys. Rev. D* **62**, 094010 (2000).
- [102] B.O. Kerbikov, hep-ph/0106324.
- [103] Y. Nambu and G. Jona-Lasinio, *Phys. Rev.* **122**, 345 (1961); **124**, 246 (1961).

[104] U. Vogl and W. Weise, *Prog. Part. Nucl. Phys.* **27**, 195 (1991); S.P. Klevansky, *Rev. Mod. Phys.* **64**, 649 (1992); T. Hatsuda and T. Kunihiro, *Phys. Rept.* **247**, 221 (1994); R. Alkofer, H. Reinhardt and H. Weigel, *Phys. Rept.* **265**, 139 (1996).

[105] H. Reinhardt, *Phys.Lett.B* **244**, 316(1990).

[106] D. Ebert, L. Kaschluhn and G. Kastlewicz, *Phys.Lett.B* **264**, 420 (1991).

[107] D. Ebert, Yu.L. Kalinovsky, L. Münchow and M.K. Volkov, *Int.J.Mod.Phys.A* **8**, 1295 (1993).

[108] A.F. Sill *et al.*, *Phys. Rev. D* **48**, 29 (1993); P. Kroll, M. Schurmann and W. Schweiger, *Z. Phys. A* **338**, 339 (1991);

[109] F. Wilczek, [hep-ph/0409168](#).

[110] U. Vogl, *Z.Phys.A* **337**, 191(1990).

[111] R.T. Cahill, J. Praschifka and C.J. Burden, *Aust.J.Phys.* **42**, 161 (1989).

[112] J. Hubbard, *Phys.Rev.Lett.* **3**, 77 (1959); R.L. Stratonovich, *Dokl. Akad. Nauk S.S.S.R.* **115**, 1907 (1957) (English translation, *Sov.Phys.Dokl.* **2**, 416 (1958)).

[113] J. Jaeckel, [hep-ph/0205154](#); J. Jaeckel and C. Wetterich, *Phys. Rev. D* **68**, 025020 (2003); J. Jaeckel, Ph.D Thesis, [hep-ph/0309090](#).

[114] J. Kapusta, "Finite-temperature Field Theory", Cambridge University Press, 1989.

[115] M.L. Bellac, "Thermal Field Theory", Cambridge University Press, 1996.

[116] D. Blaschke, D. Ebert, K.G. Klimenko, M.K. Volkov and V.L. Yudichev, *Phys. Rev. D* **70**, 014006 (2004).

[117] R.D. Pisarski and D.H. Rischke, *Phys. Rev. Lett.* **83**, 37 (1999).

[118] T.D. Fugleberg, *Phys. Rev. D* **67**, 034013 (2003).

[119] M. Alford and K. Rajagopal, *JHEP* **0206**, 031 (2002).

[120] A.W. Steiner, S. Reddy and M. Prakash, *Phys. Rev. D* **66**, 094007 (2002).

[121] M. Huang, P.F. Zhuang and W.Q. Chao, *Phys. Rev. D* **67**, 065015 (2003).

[122] S.B. Ruster, Diploma thesis, J. W. Goethe-University, 2003. S.B. Ruster and D.H. Rischke, *Phys. Rev. D* **69**, 045011 (2004).

[123] A. Mishra and H. Mishra, *Phys. Rev. D* **69**, 014014 (2004).

[124] K. Rajagopal and F. Wilczek, *Phys. Rev. Lett.* **86**, 3492 (2001).

[125] G. Sarma, *J. Phys. Chem. Solids* **24**, 1029(1963).

[126] A. Gerhold and A. Rebhan, *Phys. Rev. D* **68**, 011502 (2003).

[127] D.D. Dietrich and D.H. Rischke, *Prog. Part. Nucl. Phys.* **53**, 305 (2004).

[128] P.F. Bedaque, H. Caldas and G. Rupak, *Phys. Rev. Lett.* **91**, 247002 (2003).

[129] O. Kiriyama, S. Yasui and H. Toki, *Int. J. Mod. Phys. E* **10**, 501 (2001).

[130] M.G. Alford, J. Berges and K. Rajagopal, *Phys. Rev. Lett.* **84**, 598 (2000).

[131] W.V. Liu and F. Wilczek, *Phys. Rev. Lett.* **90**, 047002 (2003); W.V. Liu, F. Wilczek and P. Zoller, [cond-mat/0404478](#); M.M. Forbes, E. Gubankova, W.V. Liu and F. Wilczek, [hep-ph/0405059](#).

[132] E. Gubankova, W.V. Liu and F. Wilczek, *Phys. Rev. Lett.* **91**, 032001 (2003).

[133] E. Gubankova, E. G. Mishchenko and F. Wilczek, [cond-mat/0409088](#).

[134] J.R. Schrieffer, *Theory of Superconductivity* (Benjamin, New York, 1964).

[135] A. Sedrakian and U. Lombardo, *Phys. Rev. Lett.* **84**, 602 (2000).

[136] J.F. Liao and P.F. Zhuang, *Phys. Rev. D* **68**, 114016 (2003).

[137] S.B. Nam, *Phys. Rev.* **156**, 470 (1967).

[138] A.K. Geim, S.V. Dubonos, J.G.S. Lok, M. Henini, and J.C. Maan, *Nature* **396**, 144

(1998); M. Sigrist, T.M. Rice, Rev. Mod. Phys. **67**, 503 (1995); Mai Suan Li, Phys. Rept. **376**, 133(2003).

[139] H. Muther and A. Sedrakian, Phys. Rev. D **67**, 085024 (2003)

[140] E. Nakano, T. Maruyama and T. Tatsumi, Phys. Rev. D **68**, 105001 (2003); T. Tatsumi, T. Maruyama and E. Nakano, hep-ph/0312351.

[141] A.A. Abrikosov, Sov.Phys.JETP **5**, 1174(1957) [Zh. Eksp. Theo. Fiz. **32**, 1442 (1957)].

[142] I. Shovkovy, M. Hanauske and M. Huang, Phys. Rev. D **67**, 103004 (2003).

[143] H. Grigorian, D. Blaschke and D.N. Aguilera, Phys. Rev. C **69**, 065802 (2004).

[144] S. Reddy and G. Rupak, nucl-th/0405054.

[145] N.K. Glendenning, Phys. Rev. D **46**, 1274 (1992).

[146] F. Weber, *Pulsars as Astrophysical Laboratories for Nuclear and Particle Physics* (Institute of Physics, Bristol, 1999).

[147] H. Heiselberg, C.J. Pethick and E.F. Staubo, Phys. Rev. Lett. **70**, 1355 (1993); N.K. Glendenning and S. Pei, Phys. Rev. C **52**, 2250 (1995); N.K. Glendenning and J. Schaffner-Bielich, Phys. Rev. Lett. **81**, 4564 (1998).

[148] M.G. Alford, K. Rajagopal, S. Reddy and F. Wilczek, Phys. Rev. D **64**, 074017 (2001).

[149] P. Papazoglou, S. Schramm, J. Schaffner-Bielich, H. Stöcker and W. Greiner, Phys. Rev. C **57**, 2576 (1998).

[150] P. Papazoglou, D. Zschiesche, S. Schramm, J. Schaffner-Bielich, H. Stöcker and W. Greiner, Phys. Rev. C **59**, 411 (1999).

[151] M. Hanauske, D. Zschiesche, S. Pal, S. Schramm, H. Stöcker and W. Greiner, Astrophys. J. **537**, 50320 (2000).

[152] M. Alford and S. Reddy, Phys. Rev. D **67**, 074024 (2003); S. Banik and D. Bandyopadhyay, Phys. Rev. D **67**, 123003 (2003); G. Lugones and J. E. Horvath, Astron. Astrophys. **403**, 173 (2003); M. Baldo, M. Buballa, F. Burgio, F. Neumann, M. Oertel and H. J. Schulze, Phys. Lett. B **562**, 153 (2003); D. Blaschke, S. Fredriksson, H. Grigorian and A.M. Oztas, nucl-th/0301002.

[153] K. Schertler, S. Leupold and J. Schaffner-Bielich, Phys. Rev. C **60**, 025801 (1999); M. Buballa, F. Neumann, M. Oertel and I. Shovkovy, Phys. Lett. B **595**, 36 (2004).

[154] P. Nozieres, S. Schmitt-Rink, J. Low. Temp. Phys. **59**, 195(1985).

[155] E. Babaev, Int. J. Mod. Phys. A **16**, 1175 (2001); B. Kerbikov, Phys. Atom. Nucl. **65**, 1918 (2002); hep-ph/0407292.

[156] T. Matsuura, K. Iida, T. Hatsuda and G. Baym, Phys. Rev. D **69**, 074012 (2004); D.N. Voskresensky, nucl-th/0306077; D.N. Voskresensky, Phys. Rev. C **69**, 065209 (2004); I. Giannakis, D.F. Hou, H.C. Ren and D.H. Rischke, hep-ph/0406031.

[157] M. Kitazawa, T. Koide, T. Kunihiro and Y. Nemoto, Phys. Rev. D **65**, 091504 (2002); M. Kitazawa, T. Koide, T. Kunihiro and Y. Nemoto, hep-ph/0309026.

[158] H. Abuki, T. Hatsuda and K. Itakura, Phys. Rev. D **65**, 074014 (2002); K. Fukushima, hep-ph/0403091.

[159] M. Huang, P.F. Zhuang and W.Q. Chao, Commun. Theor. Phys. **38**, 181 (2002);

[160] M. Huang, P.F. Zhuang and W.Q. Chao, Commun. Theor. Phys. **34**, 91 (2000); M. Huang, P.F. Zhuang and W.Q. Chao, Phys. Lett. B **514**, 63 (2001).

[161] S. Reddy, M. Sadzikowski and M. Tachibana, Nucl. Phys. A **714**, 337 (2003); I.A. Shovkovy and P.J. Ellis, Phys. Rev. C **66**, 015802 (2002); hep-ph/0303073; P. Jaikumar, M. Prakash and T. Schafer, Phys. Rev. D **66**, 063003 (2002); S. Reddy,

M. Sadzikowski and M. Tachibana, Phys. Rev. D **68**, 053010 (2003); D. Blaschke, D. N. Voskresensky and H. Grigorian, astro-ph/0403171; D. Page, J. M. Lattimer, M. Prakash and A. W. Steiner, astro-ph/0403657; J. Kundu and S. Reddy, nucl-th/0405055; T. Schafer and K. Schwenzer, astro-ph/0410395.

[162] D.K. Hong, S.D.H. Hsu and F. Sannino, Phys. Lett. B **516**, 362 (2001); D.N. Aguilera, D. Blaschke and H. Grigorian, Astron. Astrophys. **416**, 991 (2004); A. Drago, A. Lavagno and G. Pagliara, Phys. Rev. D **69**, 057505 (2004).

[163] M. Huang, S. Scherer, H. Weber, M. Bleicher, H. Stoecker, in progress.